

April 2012

# Autonomous Multi-Robot Soccer

David E. Kent  
*Worcester Polytechnic Institute*

Frederik Emmanuel Clinckemaillie  
*Worcester Polytechnic Institute*

Quinten Reynolds Palmer  
*Worcester Polytechnic Institute*

Ryan Stephen O'Meara  
*Worcester Polytechnic Institute*

William Spencer Mulligan  
*Worcester Polytechnic Institute*

Follow this and additional works at: <https://digitalcommons.wpi.edu/mqp-all>

---

## Repository Citation

Kent, D. E., Clinckemaillie, F. E., Palmer, Q. R., O'Meara, R. S., & Mulligan, W. S. (2012). *Autonomous Multi-Robot Soccer*. Retrieved from <https://digitalcommons.wpi.edu/mqp-all/2290>

This Unrestricted is brought to you for free and open access by the Major Qualifying Projects at Digital WPI. It has been accepted for inclusion in Major Qualifying Projects (All Years) by an authorized administrator of Digital WPI. For more information, please contact [digitalwpi@wpi.edu](mailto:digitalwpi@wpi.edu).

Project Number:

AUTONOMOUS MULTI-ROBOT SOCCER

A Major Qualifying Project Report

Submitted to the Faculty

of the

WORCESTER POLYTECHNIC INSTITUTE

in partial fulfillment of the requirements for the

Degree of Bachelor of Science

in Computer Science and Robotics Engineering

by

Frederick Clinckemaiilie

---

David Kent

---

William Mulligan

---

Ryan O'Meara

---

Quinten Palmer

---

Date: 4/26/12

Approved:

---

Prof. Sonia Chernova, Major Advisor

---

Prof. Taskin Padir, Co-Advisor

Keywords:

1. humanoid robot
2. computer vision
3. localization

## **Abstract**

The goal of this project was to design and implement software to allow humanoid robots to compete in the Standard Platform League of RoboCup, a robotic soccer competition. The various modules developed by the team addressed topics in computer vision, probabilistic localization, multi-robot coordination, and off-robot visualization. By the time of the competition, the team significantly improved the robots' performance in the aforementioned topics.

## Executive Summary

RoboCup is an international scientific initiative with many objectives. The organization's original and primary focus is on developing soccer-playing autonomous multi-robot systems. The organization includes many soccer leagues, including the Standard Platform League (SPL). This league has fixed hardware, so it relies solely on the competitors' software to be successful. The Aldebaran Nao robots are currently used for the SPL competition. These humanoid robots are roughly 2 feet tall, with 21 degrees of freedom with their electric motors, 2 cameras as a primary source of input, and an Intel ATOM 1.6 GHz CPU.

The Worcester Polytechnic Institute SPL team began with the 2010 release of the University of New South Wales (rUNSWift) team's code base. The structure of the existing code is separated into four main modules: vision, localization, motion, behaviors. Each module communicates through a "blackboard" file. Modules can read from or write to the blackboard to share information with each other. The vision module takes in camera images and processes the frames to detect objects and provide robot-relative distances and headings. The localization module uses all of this robot-relative information to provide a global location for the robot and these objects. The behavior module does the decision making and controls what motions the robot runs. The motion module affects the motors to control the robot's actual movement. The WPI team previously replaced rUNSWift's localization and behaviors modules with their own code. Over the course of this project the team worked to rewrite the localization module, and to heavily modify the vision and behaviors modules, as well as develop an off-robot visualization tool for debugging and testing purposes.

The team originally intended to restructure the vision module, but given the complexity of the existing code and the time allocated to working on the vision module, the team worked more on increasing the performance of the existing module. Specifically, the accuracy of the distance and heading calculations of the various objects was targeted as an area for improvement. The team also worked to eliminate false reports of objects being detected, while still maintaining sufficient detection of objects that were present.

To replace the existing localization module the team implemented two different algorithms and a method for swapping from one to the other. The primary algorithm was a Kalman filter, which read in odometry information and robot-relative vision information to maintain and update a single robot position, while taking into account the uncertainty of the odometry and vision measurements. The secondary algorithm was a particle filter, which keeps multiple locations in working memory, which converge over time around the robot's correct position by removing low probability particles and repopulating around high probability particles. The two algorithms worked in tandem based on which algorithm was more needed—when no position estimate was given, the particle filter was in use; otherwise the Kalman filter was used to reduce impact on the processor.

The behaviors code was analyzed for effectiveness from WPI's previous competition code. The team improved whatever algorithms needed improvement, including incorporating the new data coming from the localization module, adding new robot roles to account for more soccer player behavior types, and making use of shared data broadcast over Wi-Fi between the robots.

The visualization tool was written in javascript using WebGL to graphically display the field and where the robot thought it was relative to other objects. This tool allows for 3D visualization and is accessible on any operating system that can run Google Chrome.

About halfway through the competition, a major rule change occurred in the SPL competition. Originally, one soccer goal was colored yellow and the other goal was colored blue. The rules for the 2012 competition were changed so that both goals were yellow, effectively eliminating any unique field markers for determining which side of the field the team should be scoring on and which side of the field should be defended. This particularly affected the localization module, so methods were implemented to handle this new game case.

After each module was implemented, the team carried out a number of tests to determine the effectiveness of each new module compared to the old modules. For the vision module, the accuracy of post distance detection was significantly improved, and additional object filtering to remove objects seen at unlikely distances was added. The localization module successfully implemented a Kalman filter, but due to hardware constraints the particle filter was not fully realized. The Kalman filter, along with modifications to determine which goal was which based on goalie robot team detection, was sufficient to determine a global position for the robot and preventing the robot from scoring goals on its own side of the field. The behavior module was improved for the striker and goalie role, again taking into account what would be most effective for the new same-color goal case. Also implemented in the behavior module was a support role, with the purpose of spreading the robots out on the field more effectively, but the team was unable to fully test this behavior and the role switching it required before the competition occurred. The visualization tool was completed to effectively show the positions of the robot, balls, and goals, but off-robot camera calibration was not achieved.

Overall, the new code changes were successful. The robots could more accurately detect key objects, localize based on that information sufficiently well to prevent goals on the wrong team, and the behavior module used these changes to improve the decision making required to effectively play a game of soccer. For future work on this project, the team recommends further restructuring of the vision module to incorporate a variety of object detection algorithms, extending the localization module to allow for localization based on the field lines as well as the goal posts and field edges, full implementation of role switching in the behaviors module, the addition of camera calibration to the visualization tool, and the development of a more effective walk engine and library of kicks in the as-yet-untouched motion module.

# Table of Contents

Abstract .....	i
Executive Summary.....	ii
List of Figures .....	vi
List of Tables .....	vii
List of Equations.....	vii
1 Introduction .....	1
2 Background and Literature Review.....	1
2.1 RoboCup Background.....	1
2.2 Standard Platform League Rule Changes.....	5
2.3 Vision.....	5
2.3.1 Preliminary Image Processing .....	5
2.3.2 Object Identification .....	5
2.3.3 Extraction of Object Information .....	7
2.4 Localization .....	8
2.4.1 Kalman Filter .....	8
2.4.2 Particle Filter .....	11
2.4.3 Combined Kalman Filter and Particle Filter .....	11
3 Methodology.....	12
3.1 System Overview.....	12
3.2 Vision.....	13
3.2.1 Implementation Overview .....	13
3.2.2 Testing.....	13
3.2.3 Improvements on Code .....	14
3.3 Localization .....	16
3.3.1 Kalman Filter Implementation .....	18
3.3.2 Particle Filter Implementation .....	20
3.3.3 Further Adjustments .....	24
3.4 Motion.....	25
3.5 Behaviors.....	25
3.5.1 Striker Role.....	26

3.5.2 Support Role .....	27
3.5.3 Goalie Role .....	27
1.6 Hardware Upgrades .....	27
1.6.1 New Heads .....	27
1.6.2 Camera Drivers.....	28
1.6.3 Build System.....	28
3.6 Visualization Tool .....	29
4 Results and Discussion .....	31
4.1 Initial Testing.....	31
4.1.1 Vision.....	31
4.1.2 Odometry .....	35
4.1.3 Localization .....	39
4.1.4 Time to Score .....	46
4.2 Final Testing and Individual Module Discussion .....	47
4.2.1 Vision.....	47
4.2.1: Final Post Distance Testing .....	48
4.2.2: Final Ball Distance Testing: .....	50
4.2.2 Odometry .....	52
4.2.3 Localization .....	54
4.2.4 Time to Score .....	57
4.3 Discussion of the System Performance as a Whole .....	57
5 Conclusion and Recommendations.....	58
References .....	60
Appendix A: RoboCup Standard Platform League Qualification Report.....	62

## List of Figures

Figure 1: Diagram of Aldebaran Nao.....	2
Figure 2: Standard Platform League Field Dimensions.....	3
Figure 3: Ball Radius Measurement Algorithm (Ratter et al., 2010).....	7
Figure 4: Software Architecture.....	12
Figure 5: Vision Test Positions.....	14
Figure 6: Example of Post Detection.....	15
Figure 7: Image for Viable Height-Based Post Detection.....	15
Figure 8: Image for Viable Robot Kinematic-Based Post Detection.....	16
Figure 9: Coordinate System.....	17
Figure 10: Particle Grouping.....	22
Figure 11: Particle Filter Operation.....	23
Figure 12: Data Regarding the Starting Probability Modifier's Effect on Distance Error.....	24
Figure 13: Behavior Finite State Machine.....	25
Figure 14: Visualization Tool Screenshot.....	29
Figure 15: First Architecture of Visualization.....	30
Figure 16: Final Architecture of Visualization.....	30
Figure 17: Perception Execution Order.....	31
Figure 18: The Five Trials for Robot Placement for Post Vision Testing.....	32
Figure 19: Comparisons of Distances from Posts across All Trials.....	33
Figure 20: Comparisons of Headings from Posts across All Trials.....	34
Figure 21: Difference between Observed and Real Ball Distance.....	35
Figure 22: Expected Forward Distance vs. Error.....	36
Figure 23: Expected Left Distance vs. Error.....	37
Figure 24: Linear Fit of Left Odometry Error.....	38
Figure 25: Expected Turn Angle vs. Error.....	38
Figure 26: Linear Fit of Turn Odometry Error.....	39
Figure 27: Trial 1 Trajectories and Error.....	40
Figure 28: Trial 2 Trajectories and Error.....	41
Figure 29: Trial 3 Trajectories and Error.....	42
Figure 30: Trial 4 Trajectories and Error.....	43
Figure 31: Overall X Error Data.....	44
Figure 32: Overall Y Error Data.....	45
Figure 33: Overall Theta Error Data.....	45
Figure 34: Robot Initial Position and Ball Positions for Time to Score Tests.....	46
Figure 35: Comparisons of Distances from Posts at Various Positions After Software Changes.....	48
Figure 36: Comparisons of Distances from Posts at Various Positions after Hardware Changes.....	49
Figure 37: Difference between Observed and Real Ball Distance after Software Changes.....	50
Figure 38: Difference between Observed and Real Ball Distance after Hardware Changes.....	51
Figure 39: Comparison of Differences between Observed Ball Distances for all Tests.....	51
Figure 40: Expected Forward Distance vs. Error.....	52



Figure 41: Expected Left Distance vs. Error .....	53
Figure 42: Expected Turn Angle vs. Error .....	53
Figure 43: Kalman Filter Trajectories and Error .....	56
Figure 44. Software Architecture Overview .....	64
Figure 45. Striker Behavior Stack Example.....	66

## List of Tables

Table 1: Hardware Differences Between Nao Version 3 and Version 4 .....	28
Table 2: Time to Score from Varying Ball Positions .....	47

## List of Equations

Equation 1: Kalman Filter Time Update .....	9
Equation 2: Kalman Filter Measurement Update .....	10
Equation 3: Extended Kalman Filter Time Update .....	10
Equation 4: Extended Kalman Filter Measurement Update .....	10
Equation 5: Odometry Update.....	19
Equation 6: Measurement Update .....	20

## 1 Introduction

Completion of tasks by autonomous robotics systems is a problem which presents itself in many forms. Robots that wish to complete any of a myriad of potential operations that an autonomous system may need to perform require systems to perceive the world around them, a way to perceive their place in that world, and a way to decide what actions to take. When the additional complication of coordinating with other autonomous units is introduced, the requirements for even a simple task become immense.

The Autonomous Multi-Robot Soccer team explored these issues through the design and implementation of a software system to compete in the RoboCup Standard Platform League, a robotic soccer competition involving multiple autonomous robots coordinating to play a game designed to emulate soccer on a smaller scale. The robot hardware used for this competition is standardized, which means the only difference between teams is the operation of the software they contain. This software consists of modules which allow the robot to move, process data from its cameras, use that data to determine where it is in the world, and determine what actions it should take.

The primary focus of this project was on the vision, localization, and behavior systems. Vision handles camera data, converting it into a more readily usable form for other subsystems. Localization determines where the robot is on the field. The behaviors system takes the vision and localization data and determines what the robot should do to best benefit the team, maximizing the score the team receives during a given match.

## 2 Background and Literature Review

### 2.1 RoboCup Background

RoboCup is a scientific initiative with participants from all over the world. RoboCup has four main interests: RoboCup Soccer, RoboCup Rescue, RoboCup @Home, and RoboCup Junior. RoboCup Soccer is the primary interest of the organization, and has 5 leagues: Humanoid, Middle Size, Simulation, Small Size, and Standard Platform (The Robocup Federation, 2012). The WPI Warriors team first competed in the Standard Platform League in 2011. This league has fixed hardware, so only the software can be changed. The league uses the Aldebaran Nao robots. Project Nao launched in 2004 and the Nao robots have been the robot of the SPL since 2010. The most recent release of the heads for the Nao robots is version 4, which features 2 high-definition cameras (1280x960), an Intel ATOM 1.6 ghz CPU, and wireless communications over WiFi. The body of the robots features 21 degrees of freedom (Aldebaran Robotics, 2012).

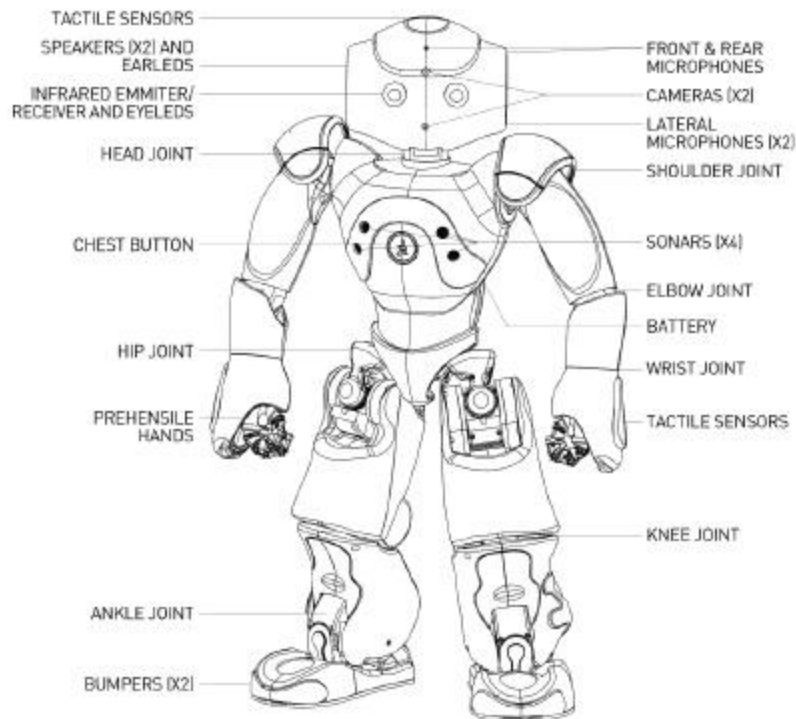


**Figure 1: Diagram of Aldebaran Nao.**

From the Aldebaran Robotics website. Retrieved 2012 from <http://www.aldebaran-robotics.com/en/Discover-NAO/Key-Features/hardware-platform.html>

The Standard Platform League has evolved its rules as the competitors have advanced their capabilities. The rules of SPL are pretty similar to the soccer game that human beings play. There are two goals at either end of a six meter long by four meter wide field. The goals are 1.4 meters wide, and are inside a 2.2 meter by 60 centimeter penalty area. There is a center circle with a diameter of 1.2 meters, as well as two penalty marks which are 1.8 meters from the back of the field in the center of the field.

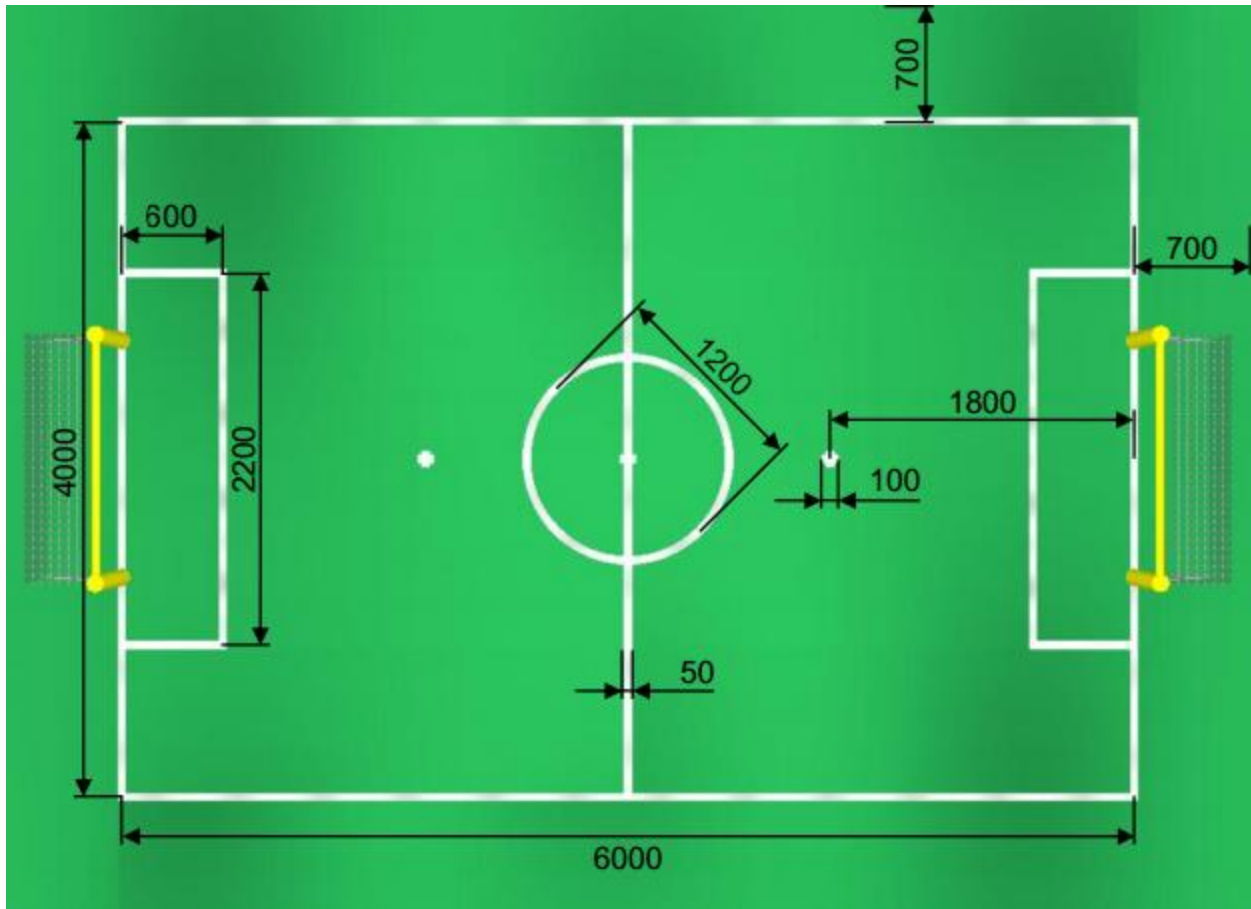


**Figure 2: Standard Platform League Field Dimensions**

From the RoboCup Standard Platform League rules website. Retrieved 2012 from [https://www.tzi.de/spl/pub/Main/WebHome/SPL\\_RuleDraft2012.pdf](https://www.tzi.de/spl/pub/Main/WebHome/SPL_RuleDraft2012.pdf)

Each team consists of four robots, and is either on team red or team blue. The teams are established on the robots by a waistband that is blue for the blue team and pink for the red team. Each team may have one goalie. The only player on a given team allowed into their own penalty area is the goalie.

There are six states during the play of a game. The game starts in an initial state, where the robots are not allowed to move any motors, but must stand upright. The robot team can be changed by hitting the left foot bumper if the robots are not listening to the GameController. The game then moves to the ready state, where the robots move to their starting positions. The ready state lasts 45 seconds. The next state is the set state. During this state the robots must wait to play. Any robot in an illegal position will be manually moved to pre-determined positions. Teams can also declare to be placed manually. If a team requests this they have all of their robots placed in less advantageous locations than if they were to automatically place themselves. The following state is the Playing state. During this state the robots effectively play a game of soccer. Robots can be moved in and out of a penalized state during the playing state. The rules for being penalized are listed in the paragraph below. After a goal is scored the robots move back to the ready state, which will then move back to the set state and then the playing

state as stated previously. When a half ends the robots move to the finished state, after which the team can physically retrieve their robots.

There are many penalties that a robot can be called for. Penalties last for 30 seconds, and when a robot is penalized it is removed from the field by a referee and must remain inactive while it is penalized. When a robot's penalty is over it is placed back on the field where the cross would intersect with the boundary line on the half of the field farthest from the ball. A list of penalties follows. Any non-goalie robot that steps into its own penalty area will be called for being an illegal defender. Any robot that holds the ball within their feet for more than 5 seconds will be called for ball holding. Any robot that is inactive for more than 20 seconds will be called for being inactive. Any robot that stays in a stance that is wider than the robot's shoulder for more than 5 seconds will be called for illegal player stance. Player pushing is the last of the penalty calls. There are many types of penalty calls. If a robot supplies enough force to knock another robot over it is called for player pushing. A robot that walks into another robot for more than 3 seconds will be called for player pushing. A robot that walks front-to-back into another robot will be called for playing pushing. A robot that is walking into a robot that is trying to get up after falling will be called for playing pushing. A robot that is attempting to get up after falling that pushes another robot that has attempted to clear the fallen robot will be called for player pushing. There are 3 exceptions to these rules. A stationary robot will not be called for pushing. A robot attempting to kick the ball will not be called for pushing, given that the referee decides it is reasonable that the kick is performed. A goalie will not be called for pushing while in the penalty area.

If a game is tied after the second half, and it is required that the game cannot end in a tie, the game will go into Penalty Kicks. There is a 5 minute break after the end of second half before the penalty kicks start. Teams can swap out to specific code for the penalty kicks. Each team gets five chances to score on the opposing team during the penalty Kicks. For penalty kicks the teams alternate between playing offense and defense. The offensive team gets one attacker and the defensive team gets one goalie. The goalie starts in the middle of the goal, and the attacking robot starts in the center of the field. The ball starts on the penalty mark. The robot has one minute to score. The goalie may not touch the ball outside of the penalty area, and the attacking robot may not touch the ball inside the penalty area. An attempt is considered a goal if the robot scores a goal on the defending team or the goalie touches the ball from outside the penalty area. An attempt is considered not a goal if the ball leaves the field, or if the attacking robot touches the ball within the penalty area, or the time expires before the ball enters the goal.

There are four human referees per game. There is a head referee who calls every penalty, signals when each half of the game starts, when each half ends, signals when a goal has been scored. All decisions made by the head referee are final. There are also two assistant referees who are responsible for moving robots as robots are penalized and un-penalized. There is also one referee who operates the GameController. This person communicates to the referees when robots are un-penalized and controls the GameController which broadcasts to the robots when a robot is penalized. A more comprehensive explanation of the rules can be found in the official RoboCup Standard Platform League Rule Draft (RoboCup Technical Committee, 2012).

## 2.2 Standard Platform League Rule Changes

Since one of the main goals of RoboCup is to advance the state of artificial intelligence through robot soccer, the rules are constantly being changed to increase the challenge of the game as competitors improve their strategies. One of the biggest changes between the 2011 competition that WPI initially competed in and the 2012 competition that this project was working towards dealt with the goal colors. Originally, goals were uniquely colored, with a blue goal on one side of the field and a yellow goal on the opposite side. This was the only unique marker on the field to distinguish which side belonged to which team. For the 2012 competition, both goals were made to be yellow, eliminating the only unique field markers. This change occurred halfway through the work on this project, and significantly affected the goals of the project and the areas focused on, which will be discussed further in the methodology section.

## 2.3 Vision

There are many ways to translate the image that a robot sees into useful information. Similarly, there are many steps required to fully processing an image. The first step is to process the raw image into regions. The second step is to identify these regions as different objects. There are various ways of doing this for each type of object. After identifying the object, the information about the object has to be extracted. Information extraction about an object depends on what type of object is being analyzed.

### 2.3.1 Preliminary Image Processing

A useful first step in image processing is to alter the image to increase both the speed and accuracy of processing the image. The robot must be able to process the image in real time, but also must identify as much correct information as possible. In a game like RoboCup, finding the point where the robot will be able to extract data as accurately as possible within a short allotted time for calculations will allow optimal game-play. With the current size of the image, the time to process the image needs to be reduced to allow the processor to work on other aspects of deciding the robot's actions (Barrett et al., 2010).

After reducing the image down to a workable size, many algorithms can be used to determine what the robot is actually looking at. One such algorithm is blob detection. To carry this out, the robot must first identify what each pixel represents. This is done most easily by applying a saliency map that maps ranges of color values to the objects that they represent.

With the salient image the robot can then identify the regions in that image. There are many forms of region detection. One form is identifying "runs" of colors that are identified by streaks of pixels of the same color. After identifying the runs along one axis (rows or columns), the runs are strung together in the other axis (columns or rows respectively). This allows any group of pixels that are the same color to be identified as a region, which can be analyzed into what type of object it is, allowing the object's properties to be extracted (Ratter et al., 2010).

### 2.3.2 Object Identification

Once an image has been sufficiently processed, the next part of the vision process involves detecting and identifying objects in the image. Many different algorithms could be used for object

identification. As such, this section will begin by exploring what object identification algorithms could be applicable to the task of identifying balls, posts, robots or field lines.

### ***2.3.2.1 Edge detection***

Edge detection algorithms can be used to reduce an image to the important edges found in it, removing a large amount of extraneous data. This algorithm is relevant to the problem of object identification because many of the objects on a soccer field are essentially lines. For example, the representation of a field line could very well be reduced to a single line, rather than an elongated rectangle. Reduction to lines would greatly simplify any further calculations that would have to be done to determine the distance to an object, and it could even simplify localization calculations that would use this data. Some objects however, such as other robots or the game ball, would not benefit as much from this approach, as a line cannot easily represent them. Another difficulty is that some lines, such as the circle found in the middle of the field, are curves, and need to be dealt with differently than the other lines found on the field. Edge detection could also have other uses, such as delimiting the size of the field to reduce the area of the image that needs to be scanned to identify field lines or balls. This was seen in team rUNSWift's implementation of an edge detection algorithm using the RANSAC algorithm, which fits a line through points while ignoring outliers, to identify the edges of the game field (Ratter et al., 2010).

The problem of edge-detection is rather non-trivial, mainly due to the fact that declaring exactly where an edge is among a smooth transition in color can be difficult. As such, there have been many offered solutions for this problem, including linear, non-linear, and best fit methods (Peli, 1982). In this case however, the task has been greatly simplified by the fact that a saliency map is generated. This saliency map means that there are only a very distinct number of colors that can actually represent relevant objects. As such, the edges will always be precise and crisp. For example, one pixel on the ball will be orange regardless of what part of the ball it is, and the neighboring one will be white if the ball lies on a field line. The change will be immediate. This means that for this situation, a version of the RANSAC algorithm will be the best solution to identify the edges found in the image.

### ***2.3.2.2 Region Detection***

Many of the algorithms used by Robocup teams for object identification include some sort of region detection. These algorithms usually work to try to identify specific regions in the image which may represent a ball, a robot, or part of a line. The algorithms used to achieve this sort of object detection are quite varied. Once again, the algorithms used for region detection can be simplified versions of commonly used region detection algorithms due to the fact that they would be used on a saliency map of the image instead of the actual image. This so greatly reduces the number of colors found in the image that it completely removes the need for using gradients to decide which pixels are part of a region and which ones are not. As such, the most relevant algorithms for this task are those already proposed by other teams, rather than more commonly discussed region detection algorithms.

The rUNSWift team uses region detection to identify lines, posts, and robots. The algorithm creates these regions by looking at each column in the image, and combining any pixels above and below of the same color into runs. These vertical runs are then stringed together with any adjacent runs

of identical color. These stringed runs are then said to be a region, and the colors of these regions are examined to identify what the region could represent (Ratter et al., 2010). The university of Texas Austin Villa Team used a similar process called blob formation to create regions. This team, however, generates the runs both vertically and horizontally. These runs are then combined to form a blob, in the form of a line running through the middle of these runs. These lines, or lineblobs, create a line which can then be used in the same way as the edges created through edge detection.

### 2.3.3 Extraction of Object Information

After the object has been identified, the robot can then determine relevant information about the object, e.g. distance and heading information that can be used for localization. Information about the ball can be determined by applying some geometry. An effective method to determine size of the ball is to select three points at random on the edge of the region of pixels identified as the ball. A line is drawn from the first point to the second point and then from the second point to the third point. The perpendicular bisectors are found to these lines. The intersection of these lines is the center of the ball. The radius of the ball can then be determined by measuring the distance from the center point to the edge of the region. This process is repeated multiple times to find the average value of the radius. The figure below illustrates the method.

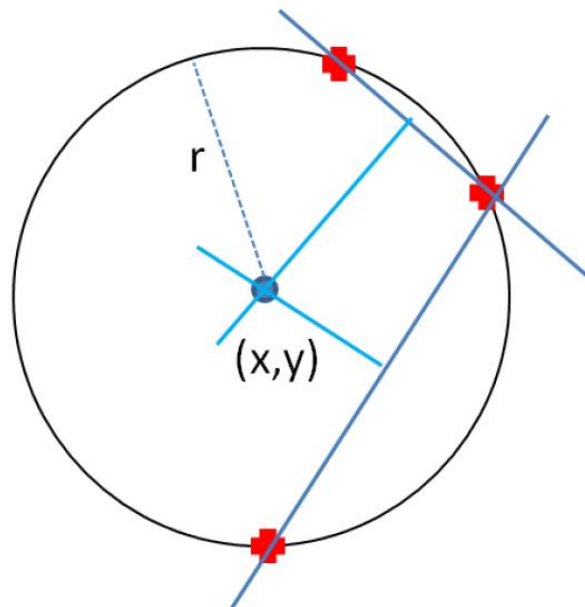


Figure 3: Ball Radius Measurement Algorithm (Ratter et al., 2010)

The post should be handled differently than the ball. There are two possible posts of each color that can be seen. Posts also differ in that it is a lot more likely that the robot will only see a portion of a post, rather than the entire post object. In the case that the robot can see the left and right boundaries of the post, then it can deduce the post's dimensions. If the robot can see the crossbar, then it can determine which post it is looking at. If the robot can see two goal posts, then it can figure out which is the left post and which is the right post (Ratter et al., 2010).



The robot also must identify the distance and heading to each object that it has identified. For the posts and the ball this is best accomplished using the kinematics chain. The kinematics chain is a method of predicting the distance of an object based on the size of a given object. The perceived size of an object can be compared to the expected size of an object. After finding the camera's height, which can be found using the joint angles, and the ground plane, which can be found from the horizon, the robot can find the distance and heading of where the vector that points to that pixel intersects with the ground plane. For the ball, the radius of the ball is used as the size attribute that is measured against the real ball size. For the post the width of the post is used if it can see the leftmost and rightmost portions of the post. When it knows the width of the post it sees it can figure out how far the post is using the same kinematics chain process explained for the ball (Ratter et al., 2010).

## 2.4 Localization

Localization has always been an interesting problem to solve in the context of the RoboCup competition. Many methods of robot localization exist, but finding the best methods to implement for individual robots with a limited field of view and limited processing capability can prove difficult. Based on the reports of teams who have had past successes in this endeavor, two strategies are prominent: Kalman filtering and particle filtering. The Nao Devils, who came in second place in the 2011 RoboCup Standard Platform League competition, are currently using a variation of Kalman filtering that uses multiple Kalman filters (Czarnetzki et al., 2010). Out of the American teams, Austin Villa uses Monte Carlo particle filtering and the UPennalizers use Kalman filtering (Barrett et al., 2010; Brindza et al., 2010). rUNSWift, the team whose code originally formed the basis of the project group's code, uses a combination of the two (Ratter et al., 2010). The following sections will describe the advantages and disadvantages of using a Kalman filter, a particle filter, and a combination of the two.

### 2.4.1 Kalman Filter

A Kalman filter is "a recursive data processing algorithm that estimates the *state* of a *noisy linear dynamic system*" (Negenborn, 2003). The term state refers to some vector of variables that can describe a system. In this case, the state of the robot would be described as the vector consisting of x location, y location, and theta orientation. Kalman filters have proven effective for robot localization as they can estimate changes in a robot's position and orientation while also including a measure of the uncertainty of its estimation. This uncertainty takes into account error in both the kinematic model of the system and the sensors of the robot.

The Kalman filter also operates under a few assumptions about the system it is implemented in. These assumptions are that the measurement noise and the model noise are independent of each other, all noise in the system is white noise and can be modeled with a Gaussian distribution, and the system is both known and linear (Freeston, 2002). Robot localization meets all of these assumptions, except that the system is often non-linear. This problem can be solved by using a variation of the Kalman filter, called the Extended Kalman Filter, which replaces the assumed linear trajectory of the system with an estimated trajectory. If updates to the Extended Kalman Filter are applied frequently, the trajectory can be assumed to be linear between each step (Negenborn, 2003). It can also account for non-linear sensor measurement data by slightly adjusting the equations of the algorithm.

The algorithm itself can be broken down into two steps. The first is the prediction step (or time update), where the state is updated to a predicted location based on a kinematic model of the system. In the case of a robot, this kinematic model is its odometry. The second step is the correction step (or measurement update), where the state is updated to reflect data from sensor measurements. In the case of a robot, this could be data from cameras, range-finding sensors, or a combination of the two (Ivanjko, Kitanov, & Petrovic, 2010). Quite useful for RoboCup, this correction step can easily be modified to include localization based on geometric beacons, which in this case are analogous to goal posts (Leonard & Durrant-Whyte, 1991).

The equations making up the algorithm are as follows, beginning with the time update equations:

$$\hat{X}_{k|k-1} = A\hat{X}_{k-1|k-1} + Bu_k \quad (1)$$

$$P_{k|k-1} = AP_{k-1|k-1}A^T + Q \quad (2)$$

Equation 1: Kalman Filter Time Update

For these equations,  $X$  represents the state vector, which in the robot's case would be  $\begin{pmatrix} x \\ y \\ \theta \end{pmatrix}_k$ . The  $k$

represents the time step of the state, and is used in the above equations to denote the time of the estimates and measurements. The vector  $u_k$  is the input vector, which in this case represents the

odometry readings since the previous update, or  $\begin{pmatrix} o_x \\ o_y \\ o_\theta \end{pmatrix}_k$ .  $A$  and  $B$  are matrices that relate the state

and input vectors to the previous state variables; more specifically they transform both vectors to the global coordinate frame, since both  $X$  and  $u$  are measured with respect to the local coordinate frame of the robot. Also, the “^” above  $X$  denotes that  $\hat{X}$  is an estimation, rather than an exact measurement. So, equation (1) calculates an estimate of the robot's pose at time  $k$  based on the pose from the previous time step ( $k-1$ ) and any odometry data received since the last update. Calculated similarly to  $\hat{X}$ , the  $P$  calculated in equation (2) represents the error covariance matrix, or the measurement of  $\hat{X}$ 's error mentioned at the beginning of this section.  $Q$  represents the noise covariance matrix of the model, and is often determined experimentally. The higher  $Q$  is, the less trusted the measurements are; likewise a  $Q$  close to zero means the expected noise of the model is low, and therefore the update is trusted to be accurate.

Once the time update is complete, if the robot has some measurement input at the current time step, the measurement update is performed using the following equations:

$$J_k = P_{k|k-1} C^T (C P_{k|k-1} C^T + R)^{-1} \quad (3)$$

$$\hat{X}_{k|k} = \hat{X}_{k|k-1} + J_k (Y_k - C \hat{X}_{k|k-1}) \quad (4)$$

$$P_{k|k} = (I - J_k C) P_{k|k-1} \quad (5)$$

#### Equation 2: Kalman Filter Measurement Update

These equations introduce some new variables.  $Y$  represents the measurement vector.  $C$  is a matrix relating the measurement vector to the state vector, similar in function to matrices  $A$  and  $B$  above.  $R$  is similar to  $Q$  except that instead of representing the noise of the kinematic model, it represents the noise covariance matrix for the measurement.  $J$  is the Kalman gain, used to determine to what extent the measurement update can be relied upon. So, equation (3) calculates the Kalman gain, which depends on the error covariance matrix of the time update and the inverse of the measurement covariance matrix. It is then used in the actual measurement update to the state performed in equation (4), where a higher or lower  $J_k$  means the update will be scaled to have more or less importance depending on the confidence of the time update and the measurement accuracy. Finally, equation (5) updates the error covariance matrix  $P$  to account for any changes to the accuracy of the state vector brought about by the measurement update.

The Extended Kalman Filter uses similar equations, with a few slight adjustments:

$$\hat{X}_{k|k-1} = A \hat{X}_{k-1|k-1} + B u_k \quad (1)$$

$$P_{k|k-1} = A P_{k-1|k-1} A^T + Q \quad (2)$$

#### Equation 3: Extended Kalman Filter Time Update

$$C_k = \left. \frac{\partial h}{\partial X} \right|_{X=\hat{X}_{k|k-1}} \quad (3)$$

$$J_k = P_{k|k-1} C_k^T (C_k P_{k|k-1} C_k^T + R)^{-1} \quad (4)$$

$$\hat{X}_{k|k} = \hat{X}_{k|k-1} + J_k (Y_k - h(\hat{X}_{k|k-1})) \quad (5)$$

$$P_{k|k} = (I - J_k C_k) P_{k|k-1} \quad (6)$$

#### Equation 4: Extended Kalman Filter Measurement Update

The time update is unchanged. The measurement update, however, uses a varying  $C$  (now denoted  $C_k$ , to show that it varies with the time step).  $C_k$  is determined by the function  $h$ , which describes the non-linearity of the sensor data used for the measurement update. Non-linear trajectories are handled by making updates over short time steps, so that any changes to the robots position can be assumed to be linear. Aside from these changes, the equations work the same way, and the Kalman filter is extended for use with non-linear data.

Kalman filtering has two large downsides, however. Since the algorithm is based directly on the previous location information, it requires an accurate initialization. Without knowing its initial position and orientation, a robot's localization updates are essentially starting from a faulty guess of its pose. This initial error can be difficult to recover from. Similarly, as small errors propagate from one update to the next, the robot can eventually reach a state of high error; since each update is so dependent on the previous update, the robot may be unable to recover an accurate pose estimate (Ratter et al., 2010).

#### **2.4.2 Particle Filter**

Particle filtering is a process by which particles are spread over an environment which represent possible positions and headings for the robot. Each particle also contains a probability of how likely each pose is. The probabilities associated with each particle are adjusted according to observed features, and low probability particles are removed, while high probability particles are multiplied (Martinez-Gomez, Jimenez-Picazo, & Garcia-Varea, 2009). Particle filters are best applied where uncertainty should be preserved, as it is tracked by multiple groups of particles in the environment.

An important assumption that must be met when using particle filters is that a model of the environment exists. This model must be able to accurately determine the probability of the robot being at various locations based on sensor data. This leads to a secondary assumption that the entirety of the area in which the robot is operating can be represented in software, including major features which are used to determine position (Rekleitis, 2004).

Particle filters operate by a principle of prediction and refinement. The algorithm starts by spreading particles across the environment with equal probabilities. It then processes sensor input and compares it to the known environment, using that data to adjust the probabilities of the particles. It then resamples the particles, eliminating low probability particles and multiplying high probability particles. Finally, the list of particles is further refined by repeating the sensor data processing and resampling steps (Rekleitis, 2004).

Particle filters excel when used in known environments where major features may be used to determine position. Such systems do not need an initial position to base calculations off of, and are well suited for situations where the robot has just been introduced into the environment.

A major downside to the particle filter approach is the inability to effectively determine positions in open environments. Open environments are extremely hard to convert into a virtual representation effectively. Other environments with an overabundance of features are also problematic—with too many matches for possible positions, the certainty of determining the actual position of the robot is much lower. Another downside that is important to the RoboCup problem is that they are computationally intensive if a large number of particles are used. To implement a particle filter on a Nao robot, simplifications would need to be made.

#### **2.4.3 Combined Kalman Filter and Particle Filter**

Using a combination between Kalman filtering and particle filtering can eliminate many of the downsides from both algorithms (Ratter et al., 2010). Beginning localization with a particle filter can quickly narrow a robot's initial pose to a reasonable possibility. Localization can then switch to using a

Kalman filter primarily. This fixes the Kalman filter’s weakness of finding an initial position, while also using the particle filter as little as possible to reduce the performance impact on the system. Similarly, when the Kalman filter’s error propagates to the point that the robot loses its position, the particle filter can be run for a short period of time to determine a more correct position to restart the Kalman filter on.

### 3 Methodology

#### 3.1 System Overview

Since the team originally adopted the rUNSWift code as the basis for the project, the software architecture is similar to rUNSWift’s original software architecture. An diagram of the software architecture is shown below.

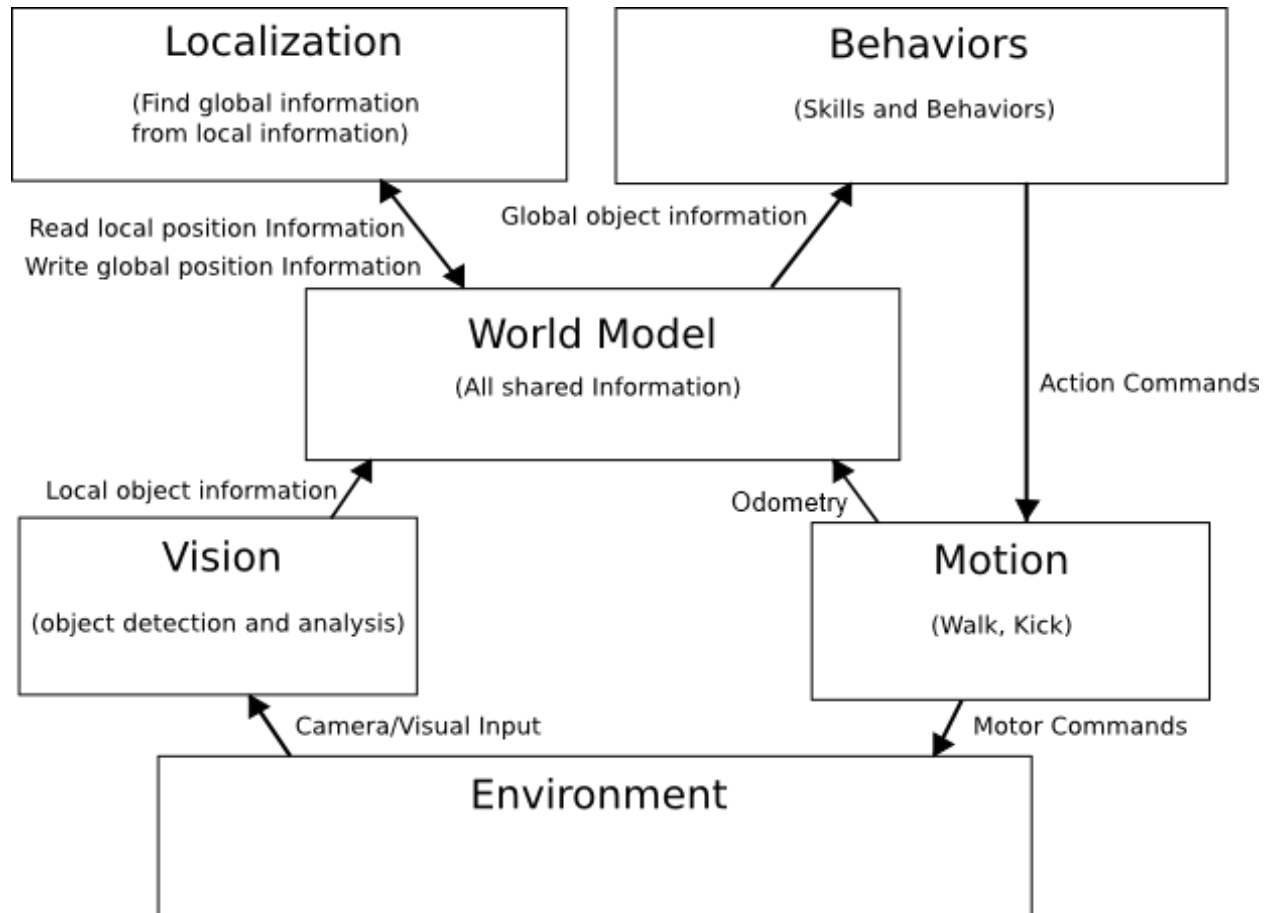


Figure 4: Software Architecture

The four primary modules that make up the software are Vision, Localization, Motion, and Behaviors. Each module shares information with the other modules through the World Model, which is implemented using a “blackboard” analogy where relevant modules can either read from or write to different sections of the blackboard.

The rules of the competition state that one module may be left unchanged from another team's code, an additional module may be kept if it is significantly modified, and all other modules must be completely rewritten. The team chose to keep rUNSWift's Motion module, modify the Vision module, and create original Localization and Behaviors modules. Below is a description of the implementation of each module, as well as the development processes used.

## 3.2 Vision

The vision module was selected as the module that would only be altered instead of being fully replaced. As such, it remains heavily based on the rUNSWift implementation. The following process was used to modify the vision module. The rUNSWift vision module was first tested to determine its accuracy in measuring both the angles and distances of goal posts and balls. Next, the code was examined in detail to gain a better understanding of it, and the goal post and ball detection algorithms were improved wherever possible. Finally, similar accuracy tests for the vision module were performed to measure improvements in accuracy. Each step will be discussed below, beginning with an overview of how the rUNSWift team implemented their vision module.

### 3.2.1 Implementation Overview

The implementation of the vision module feeds the raw image from the raw camera into the Vision class, which runs that image through the vision pipeline. The pipeline calls a series of other classes to process and analyze the frame to obtain information about different objects found in the frame, and to calculate their positions and orientations relative to the robot.

For the first step in this task, the module first creates a saliency map of the raw image. This map is a compressed version of the raw image with a calibration file applied to it, reducing it to a number of predetermined colors, such as goal-post yellow, goal-post and robot blue, robot red, field line and robot white, field green, ball orange, and background. All other colors are removed from the image to make the process of analyzing the file easier.

The Vision class then uses the fieldEdgeDetection class to determine the edges of the fields, and the regionBuilder class to group regions with similar colors into different regions, such as robot or post regions. The regions are then analyzed depending on their type. For example, ball regions are processed using the ballDetection class, robot regions by the robotDetection class, and goal regions by the goalDetection class. Each of these classes is tasked with determining the position and orientation of an object relative to the robot. This includes calculating its distance and its angle from the information gathered on the region. Then, this data is used to apply a series of sanity checks to ensure the results are actually plausible. If they are, the position of each object, be it a ball, another robot, or a goal post, is written to the blackboard for use in the localization and behaviors modules.

### 3.2.2 Testing

The capabilities of the vision module were thoroughly tested prior to making any changes, to both determine what most needed improvement, and to be able to quantitatively measure the progress made in this project. The testing was divided into two different sets of tests, one for post detection and the other for ball detection.

The first set of tests focused on goal post detection. This was done by picking several different positions on the field, having the robot face the goal from these positions, and recording both the angle and the distance of any post the robot was able to see. The positions of the robot for these tests are shown below.

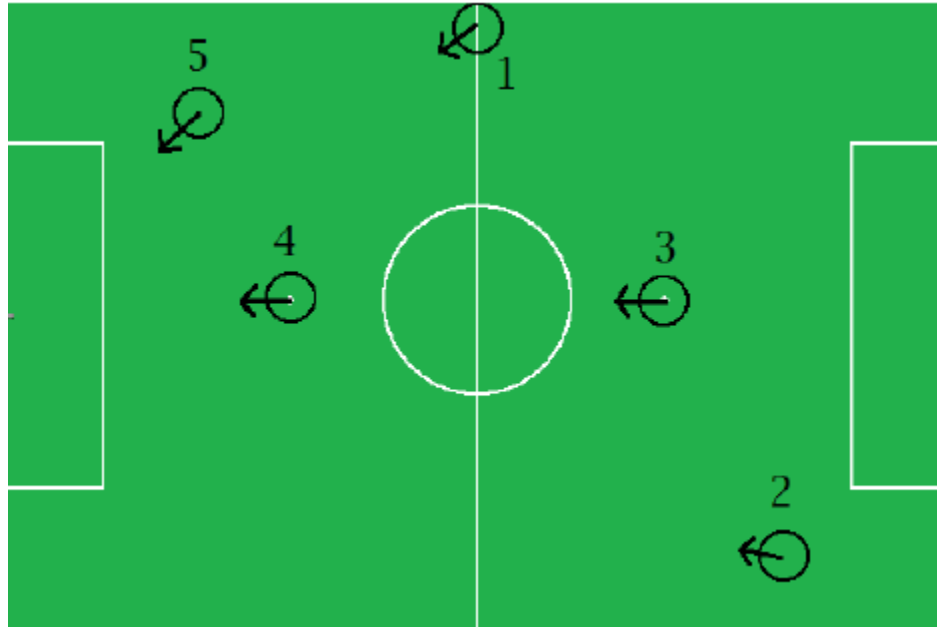


Figure 5: Vision Test Positions

The second set of tests determined the accuracy of distance measurements for the ball detection. For this, a ball was placed at various distances away from the robot and the perceived distance was compared with the actual distance. The distances used for this test were 500 mm, 1000 mm, 1500 mm, 2000 mm, 3000 mm, and 4000 mm. The results were then graphed and analyzed. The results of this testing, as well as the goal post testing, can be found in the Section 4.1.1 of the Results section of this report.

### 3.2.3 Improvements on Code

After the testing phase, it was determined that additional improvements were required for both the goal detection and ball detection to increase their accuracy.

For the goal detection, the first step was to modify the values for the expected height and width of the pole. This was required because the poles used during testing are not quite equal to those used in competition, which can provide inaccurate measurements. Furthermore, it was found that the program calculated the distance away from a post using only the post's width. For example, in the figure below, the light blue box marking a detected post region is drawn around the post, and the width of that rectangle is used to calculate the distance to the robot.

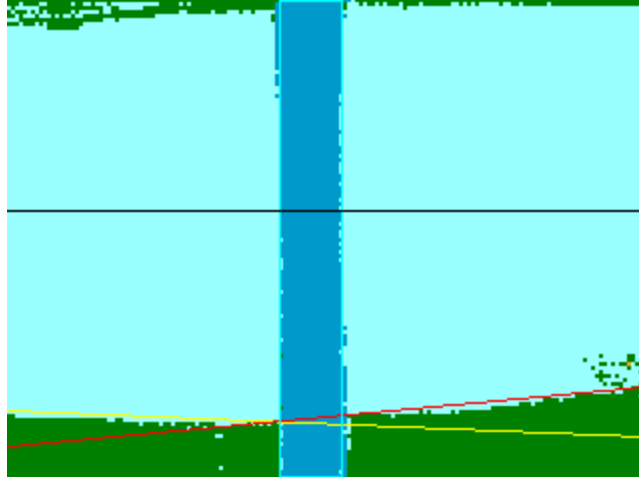


Figure 6: Example of Post Detection

This had to be changed because the robot often gets faulty width readings depending on the blur caused by head motion during scans. Since the post is a relatively thin object, this blur can greatly effect distance measurements. As such, additional methods of measuring the distance to a post were implemented.

The first one of these methods was to use the height of the post as a way of measuring the distance, in a similar fashion to using the width. In theory, this measurement should be much more reliable, as the height is greater than the width, and as such it is less likely to be affected by the movement of the robot's head. However, this method requires the entire post to be in the image, making it only viable for images like the one shown in the figure below. Even though this does not cover situations where the robot is close to the posts, it can be used in almost all situations when the robot is mid-field or further back, which originally had the greatest error when only width measurements were used.

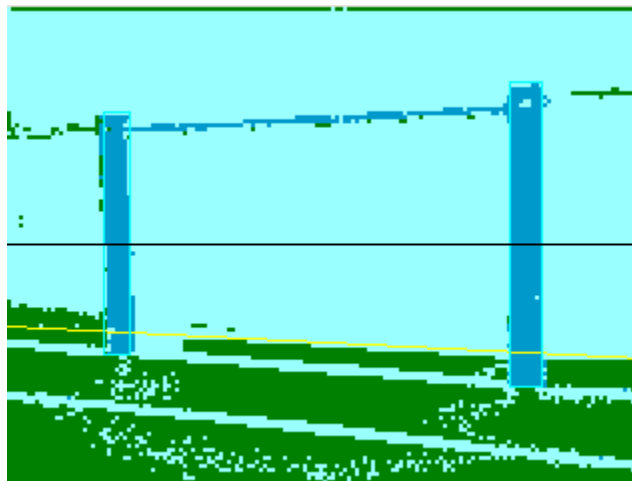


Figure 7: Image for Viable Height-Based Post Detection



A third method was implemented to derive the distance between the robot and a post when only the bottom of a post is seen. The theory is that if the robot kinematics are known, then it is possible to map any pixel from a camera image to a distance, as long as that pixel marks a point on the floor. In the RoboCup soccer situation, a green pixel within the field lines is guaranteed to be a point on the floor. As such, finding the distance to the pole is just a matter of looking for a field-green pixel right under a pole and using the robot kinematics to map that pixel to an actual distance. These calculations are made easier by the fact that the rUNSWift code already had a method of handling the robot kinematics. The only downside to this technique is that it must find green pixels right under a pole to be useful, so this method is highly dependent on a good calibration file. The following figure demonstrates the kind of image where this method can be used.

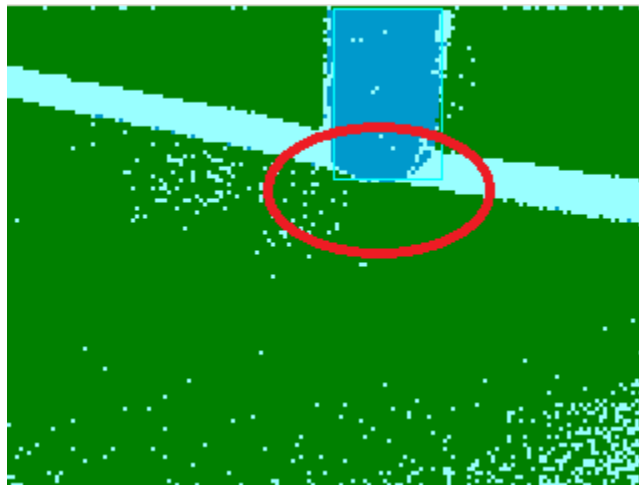


Figure 8: Image for Viable Robot Kinematic-Based Post Detection

Most of the pole is not in the image, so the height measurement cannot be used. However, the bottom of the pole has many green pixels right under it, making it very likely that using one of these to calculate the distance to the goal will be accurate.

The two new methods are expected to be much more accurate than the width based calculation that was used before for the reasons described above. As such, the height method was prioritized above the other two methods, with the kinematics methods prioritized over using the width.

The same principle of using the robot kinematics and a field pixel at the bottom of a post can also be applied to ball detection. The current ball detection algorithm is based on using the radius of the ball to estimate its distance. This method was, like the goal post width, highly susceptible to error from camera blur caused by camera scanning movements and bad calibration files. However, if green pixels can be found under the ball, the position of these pixels can be used in conjunction with the robot kinematics information to determine the distance to the ball.

### 3.3 Localization

The localization module was completely rewritten from the module used during the 2011 RoboCup competition. The new module incorporates both particle and Kalman filtering to keep track of

the robot's position, similar in purpose to the localization system used by the rUNSWift team. However, both the particle filter and the Kalman filter required significant adjustment from the theoretical models discussed previously to work for this particular problem.

Both filters were implemented so that they could turn on and off at any time the robot chose too. As such, they had to share a coordinate system. The figure below shows the coordinate system that both filters use. The coordinates are implemented relative to which team the robots are playing on. This allows for faster to change and easier to understand code in the behavior module, which often undergoes last-minute adjustments during competition. A robot's position is defined as  $(x, y, \theta)$ , where  $x$  represents the position along the field width,  $y$  represents the location along the field length, and  $\theta$  represents the robot's orientation with respect to the x-axis:

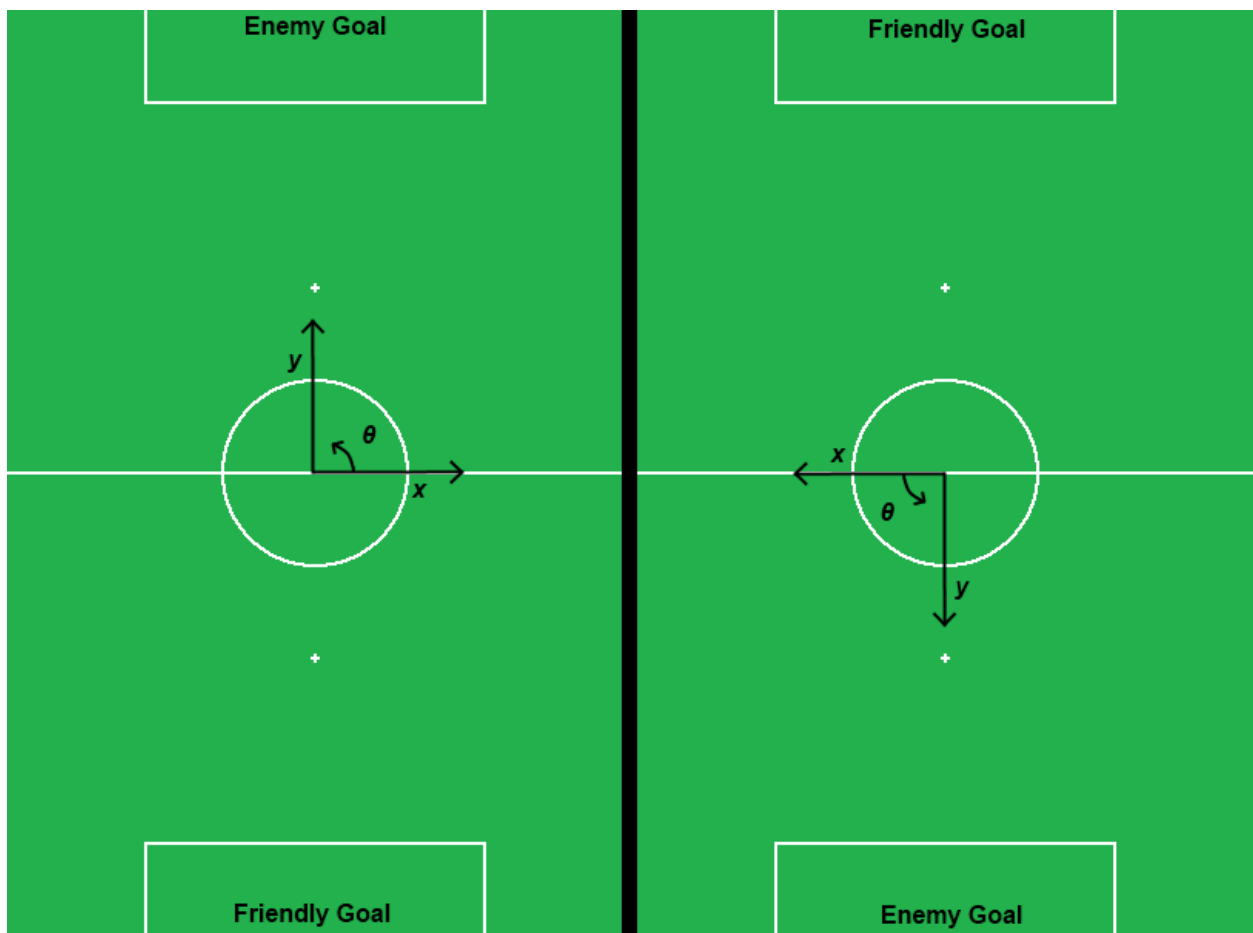


Figure 9: Coordinate System

Each filter also includes a measurement of how accurate the robot believes its current position to be, which determines when the current filter in use should be switched out. The Kalman filter uses a measurement of variance, and switches to the particle filter when the variance is high (i.e. when the robot is highly unsure of its position). The particle filter uses a probabilistic measurement of how correct its position is, and will switch to the Kalman filter when the probability is high (i.e. when the

robot is more sure of its position). This switching criteria allows the localization module to use the less resource-intensive Kalman filter whenever the robot is sure of its position, but will allow the use of the more resource-intensive particle filter in critical situations when the robot becomes lost.

Similar to the vision module development process, the localization module development incorporated many tests. The module used by the WPI RoboCup team in 2011 was first tested to use as a basis of comparison to determine how well the new implementation worked. This also provided a quantifiable way of measuring the progress of this project. The results of the initial and final tests can be found in sections 4.1.3 and 4.2.3 of the Results and Discussion section of this paper.

The following sections describe the implementation of the Kalman filter and the particle filter in more detail.

### 3.3.1 Kalman Filter Implementation

The implementation of the Kalman filter follows the same algorithm as described earlier, but with some modifications and additions to work for the problem of robot localization on a soccer field. The algorithm begins with the Kalman filter time update.

The robot's odometry is a decent, and constant, indication of the robot's positional change over time, so the time update was modified to become an odometry update. The basic equations remain in the form:

$$\begin{aligned}\hat{X}_{k|k-1} &= \hat{X}_{k-1|k-1} + Bu_k \\ P_{k|k-1} &= AP_{k-1|k-1}A^T + Q\end{aligned}$$

$\hat{X}$  represents the robot's location  $\begin{pmatrix} x \\ y \\ \theta \end{pmatrix}_k$ ,  $u$  represents the change in odometry  $\begin{pmatrix} o_x \\ o_y \\ o_\theta \end{pmatrix}_k$  since the last

update, and  $P$  and  $Q$  represent the covariance matrices  $\begin{bmatrix} x_{\text{var}} & 0 & 0 \\ 0 & y_{\text{var}} & 0 \\ 0 & 0 & \theta_{\text{var}} \end{bmatrix}$ . The matrix  $A$  is replaced

with the identity matrix, since the current location estimate does not need any matrix transformation to relate to the previous location estimate. Since the change in odometry is measured in a coordinate frame relative to the robot, however, it needs to be transformed to the global coordinate frame, so the matrix  $B$  is set to a transformation matrix for that purpose. Covariance values for the matrix  $Q$  were determined experimentally based on the accuracy of the odometry. The final equations are as follows:

$$\begin{pmatrix} x \\ y \\ \theta \end{pmatrix}_{k|k-1} = \begin{pmatrix} x \\ y \\ \theta \end{pmatrix}_{k-1|k-1} + \begin{bmatrix} -\cos\left(\frac{\pi}{2}-\theta\right) & \sin\left(\frac{\pi}{2}-\theta\right) & 0 \\ -\cos(\pi-\theta) & \sin(\pi-\theta) & 0 \\ 0 & 0 & 1 \end{bmatrix} \begin{pmatrix} o_x \\ o_y \\ o_\theta \end{pmatrix}_k$$

$$\begin{bmatrix} x_{\text{var}} & 0 & 0 \\ 0 & y_{\text{var}} & 0 \\ 0 & 0 & \theta_{\text{var}} \end{bmatrix}_{k|k-1} = \begin{bmatrix} x_{\text{var}} & 0 & 0 \\ 0 & y_{\text{var}} & 0 \\ 0 & 0 & \theta_{\text{var}} \end{bmatrix}_{k-1|k-1} + \begin{bmatrix} .002 & 0 & 0 \\ 0 & .002 & 0 \\ 0 & 0 & .002 \end{bmatrix}$$

Equation 5: Odometry Update

Also, as a modification from the time update equations, the x and y values for the noise covariance matrix  $Q$  are set to zero if there is no change in both the x and y odometry, and similarly the  $\theta$  value is set to zero if there is no change in the  $\theta$  odometry. This way, the covariance increases linearly only when the robot is actually moving, rather than increasing constantly as time passes. This represents the behavior of the odometry error, which increases additively as the robot continues moving for long periods, but does not change when the robot is standing still.

The second part of the Kalman filter algorithm is the measurement update. The implementation of this part of the algorithm incorporates measurement updates only when one or more goal posts are seen by the robot. Again, it follows the theoretical equations of the Kalman filter:

$$\begin{aligned} J_k &= P_{k|k-1} C^T (C P_{k|k-1} C^T + R)^{-1} \\ \hat{X}_{k|k} &= \hat{X}_{k|k-1} + J_k (Y_k - C \hat{X}_{k|k-1}) \\ P_{k|k} &= (I - J_k C) P_{k|k-1} \end{aligned}$$

Here  $Y$  represents the new position calculated from the vision information about the post(s) seen by the robot.  $J$  represents the Kalman gain,  $C$  is a transformation matrix, and  $R$  is a covariance matrix. The other variables are the same as in the odometry update implementation. For the implementation of the measurement update, the equations can be simplified by replacing  $C$  with the identity matrix. As with matrix  $Q$  in the odometry update, the error values of matrix  $R$  were determined experimentally based on the accuracy of the vision module. The final equations for the measurement update are as follows:

$$\begin{aligned} \begin{bmatrix} J_x & 0 & 0 \\ 0 & J_y & 0 \\ 0 & 0 & J_\theta \end{bmatrix}_k &= \begin{bmatrix} x_{\text{var}} & 0 & 0 \\ 0 & y_{\text{var}} & 0 \\ 0 & 0 & \theta_{\text{var}} \end{bmatrix}_{k|k-1} \left( \begin{bmatrix} x_{\text{var}} & 0 & 0 \\ 0 & y_{\text{var}} & 0 \\ 0 & 0 & \theta_{\text{var}} \end{bmatrix}_{k|k-1} + \begin{bmatrix} [.1, .5] & 0 & 0 \\ 0 & [.1, .5] & 0 \\ 0 & 0 & [.1, .5] \end{bmatrix} \right)^{-1} \\ \begin{pmatrix} x \\ y \\ \theta \end{pmatrix}_{k|k} &= \begin{pmatrix} x \\ y \\ \theta \end{pmatrix}_{k|k-1} + \begin{bmatrix} J_x & 0 & 0 \\ 0 & J_y & 0 \\ 0 & 0 & J_\theta \end{bmatrix}_k \left( \begin{pmatrix} Y_x \\ Y_y \\ Y_\theta \end{pmatrix}_k - \begin{pmatrix} x \\ y \\ \theta \end{pmatrix}_{k|k-1} \right) \end{aligned}$$

$$\begin{bmatrix} x_{\text{var}} & 0 & 0 \\ 0 & y_{\text{var}} & 0 \\ 0 & 0 & \theta_{\text{var}} \end{bmatrix}_{k|k} = \begin{bmatrix} 1-J_x & 0 & 0 \\ 0 & 1-J_y & 0 \\ 0 & 0 & 1-J_\theta \end{bmatrix} \begin{bmatrix} x_{\text{var}} & 0 & 0 \\ 0 & y_{\text{var}} & 0 \\ 0 & 0 & \theta_{\text{var}} \end{bmatrix}_{k|k-1}$$

**Equation 6: Measurement Update**

The biggest change to the measurement update equations is that the measurement error covariance matrix  $R$  is set dynamically. The values are set from a range depending on how accurate a position can be drawn from the vision information. For example, if both posts are clearly seen, the error value is set to the low end of the range at .1. In the worst case, if only one post is seen at a far distance, the error value is set to .5, the high end of the range.

The above equations represent the majority of the Kalman filter implementation, but there are also a few additions to improve its operation. One addition is bounds checking. Since the field size is known, and since robots are penalized and removed from play if they step too far off the field, a reliable set of bounds can be defined to check the robot's position against. Between Kalman filter updates, the localization module checks to see whether the robot has moved outside of the bounds. If so, the Kalman filter moves the estimated position onto the field boundary and increases the appropriate variances values in the matrix  $P$ .

The other notable addition is in the Kalman filter initialization. Whenever the localization module switches to using the Kalman filter, the variance values in  $P$  are set to a medium value, even if the robot was very sure of its position from the particle filter. This fixes an observed behavior of the robot where the localization updates too slowly, because the robot perceives its position as nearly perfect.

### 3.3.2 Particle Filter Implementation

The particle filter in this system was designed and implemented to fulfill the specific need for a method which performed well when there is no reliable data on the robot's initial position. Its main strength is the lack of assumptions about previous position during calculation of the current position. This feature allows it a better chance of giving a correct position at the beginning of the game and when the robot has been penalized. The main weakness of a particle filter is that it is processor intensive, and easily affected by erroneous sensor data. For this reason, once a position for the robot has a certain probability, localization is passed off to the Kalman filter.

#### 3.3.2.1 Operation

The particle filter operates by maintaining a list of particles, each particle consisting of an x coordinate, y coordinate, theta value, and probability. The system executes a set of code every program loop which evaluates sensor data and adjusts the probability of each particle accordingly. Afterwards, the points with the lowest probability are discarded, to be replaced by new particles. The new particles are in an area around the particles with the highest probability.

The first operation performed by the filter each iteration is to adjust all particles for odometry data. The odometry data is processed, and the data of each particle is updated to reflect the robot's movement. This could be accomplished by allowing the probabilities of the previous particles to decrease, and new particles closer to the actual position to be generated. However, this requires more time and processing to accomplish, and updating each particle with movement data accomplishes the same goal in a more efficient manner. After these adjustments are made, the filter checks that all particles are still within the bounds of the workspace, and removes any particles which do not meet these criteria.

Following adjustments for odometry, each particle's probability is updated based on sensor data. The system calculates the expected distance and heading from each particle to the sighted goal posts, and compares it to the measured heading and distance provided by the vision system. In addition to the modifications by the sensor data, each particle's probability is changed based on the direction its theta value indicates. Particles with a theta value facing the sighted goal posts have their probability increased, and particles with a theta value facing away from the sighted post have their probability decreased. The team association of the sighted goal posts is determined by the goalie sighted within the goal.

The sensor data given to the particle filter had the potential to be erroneous in many ways. Testing indicated the possibility of invalid ranges, sighting only one post, and being unable to identify which team a goal belonged to. This was mitigated by reducing how much the probability of the particles was adjusted based on the given data when one of these conditions was detected.

Following the evaluation of sensor data, the filter trims the lowest probability particles from the list. These particles are then replaced by new particles, whose x, y, and theta values are determined by the positions of the highest probability particles. Initially, there were problems with the filter "settling" on a few high probability particles, to such a degree that the newly introduced particles were always eliminated as the "lowest probability" in the set. This was mitigated by adjusting the probabilities of existing particles such that their average is equal to the probability assigned to new particles. As a further probability modification, the probabilities of all particles were rescaled each iteration to be in the expected range of zero to one.

The bounds for creating new particles are calculated by recognizing groups of particles using a density based algorithm, which isolates clusters of high probability particles, allowing a more efficient placement of newly generated particles.



**Figure 10: Particle Grouping**

The figure above shows the grouping of particles (blue) into boundary sets (red). The filter generates several boundary sets, narrowing them down and combining them. If more than two sets remain after this process has been completed, the average probability of the set is used to determine which two sets are selected. The reason for using two sets lies with the rule change that caused both goals to be the same color; without seeing a goalie, the localization module should recognize that there are two possible positions for the robot on the field, in the same relative position to each goal.

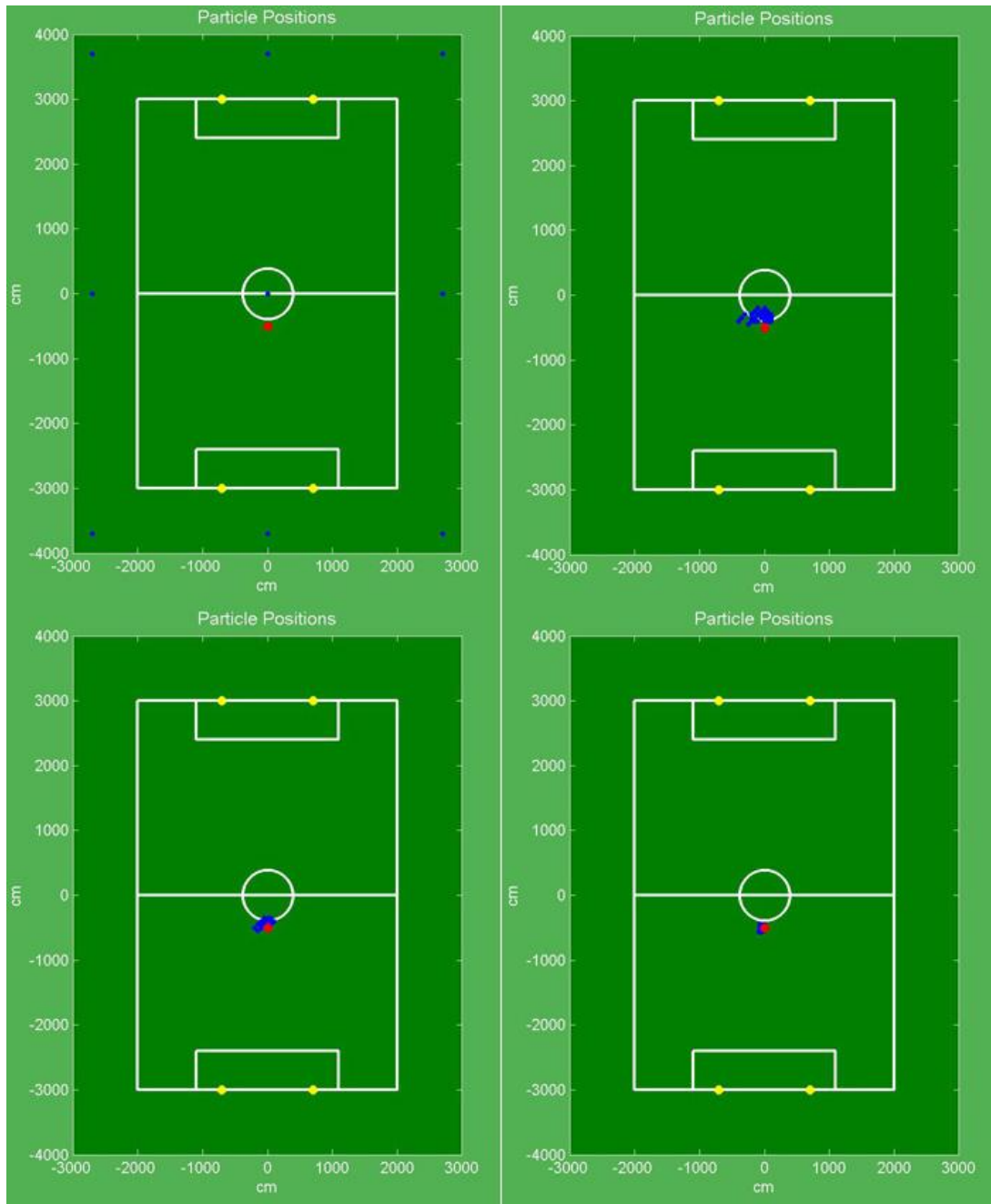


Figure 11: Particle Filter Operation

The figure above illustrates a time lapse of particles (blue) coalescing around the actual robot position (red) using vision data giving distance and heading data to the goal posts (yellow). The particles start out spread across the field in the x, y, and theta dimensions, with an initial probability of fifty percent. The particle filter's operation results in the particles slowly grouping around the highest probability location for the robot, over a period of several localization routines.



### 3.3.2.2 Tuning

Although the filter itself is robust, its internal constants must be tuned in order to operate at peak capacity. Several methods were used to determine the optimum value for each constant. The first was a rough adjustment and test procedure, which was extremely slow. Next, an automated simulation and testing setup was tried. This procedure measured distance error, theta error, number of loops to settle, and the maximum number of loops on a value besides the returned value. This data was recorded for 25 separate points, changing the value of the variable being tested each time. All variables which effect particle probability were tested in this manner. The error data of the points for each value of the variable was averaged and graphed, and these graphs were used to determine the value used for each variable.

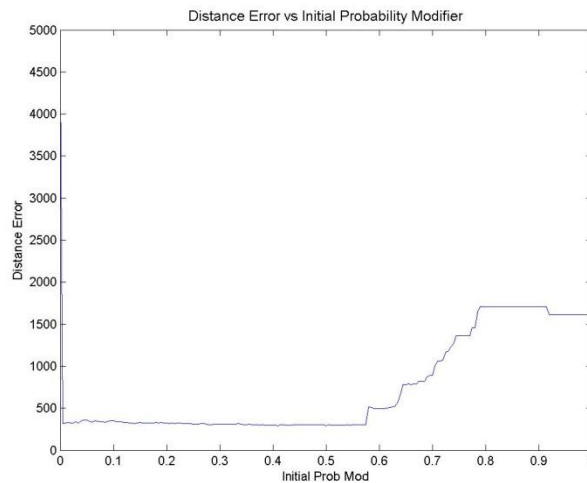


Figure 12: Data Regarding the Starting Probability Modifier's Effect on Distance Error

### 3.3.3 Further Adjustments

Due to a change in the competition rules, the previously different goal colors were changed to be the same color, removing the only unique field objects. This significantly affected localization, since the robots could no longer determine whether the goal posts seen by vision belonged to the enemy team or the friendly team.

The Kalman filter, since it keeps track of a previous position, could handle this change without too much difficulty. As long as odometry error propagation remained low enough that the robot did not become turned around by 180 degrees, the robot could determine which goal it was looking at for use in the Kalman filter measurement update. The particle filter, on the other hand, could not determine which goal was which, and this resulted in the particle filter determining two positions of similar likelihood on opposite sides of the field.

To fix this problem, the robot used robot detection in conjunction with vision information about the goal posts to determine whether there was a goalie in the goal. If a goalie was detected, the goal type was determined based on the goalie's team color. If no goalie was detected, the localization module relied on past information to determine which goal was which as best as possible.

### 3.4 Motion

The motion module was left relatively untouched from rUNSWift’s original code. A few small additions were added to improve the performance of the robots, however. First, new motions were added for performing various kicks and for getting up after falling down. These motions were implemented essentially as key-framed animations which can be run un-interrupted from the behaviors module. The second addition was a simple adapter class for the odometry that allows linear adjustments including scaling and offsets to the odometry output, which were determined via odometry testing for each individual robot.

### 3.5 Behaviors

The Behavior module is implemented as a finite state machine, where each state has a behavior state associated with it. To give an idea of what a behavior state can be, some example states are “Walk to Ball”, “Find Ball”, and “Kick Ball”. The state machine also maintains a notion of roles. These roles are represented as clusters of states. The team currently uses three roles: Striker, Goalie, and Support. The striker role plays an offensive role, with the main objective of scoring a goal. The Goalie is responsible for defending the goal and preventing the enemy team from scoring. The Support role is responsible for either helping the striker score, or the Goalie prevent the other team from scoring, depending on the supporter’s field position. This state machine has states that correspond to these roles. Each role has a branched stack-like structure that dictates how the role should perform its task. The robots can be called upon to switch to another role if another robot has been removed from the field. Furthermore, the robots often switch between the striker and support roles depending on their respective distances to the ball.

Below is an overview of the full state machine for the Behavior module.

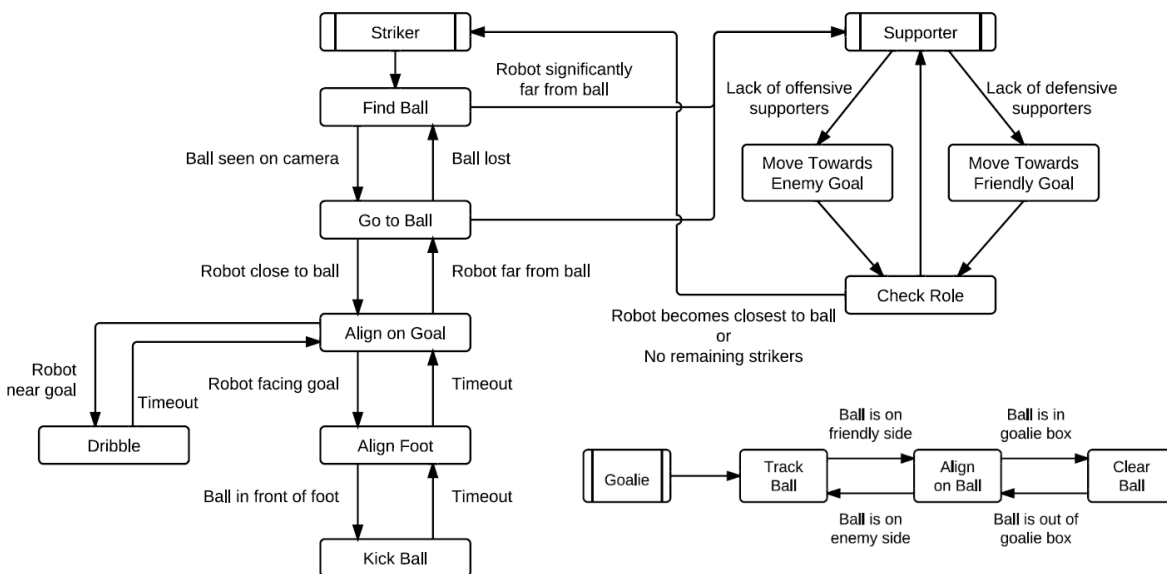


Figure 13: Behavior Finite State Machine

Each role will be discussed in detail in the following sections.

### 3.5.1 Striker Role

The striker has six states that it uses to score on the enemy goal: FindBall, GotoBall, AlignGoal, Dribble, AlignKick, and KickBall. The operation of each state and how each state can be reached is described below.

The striker starts in the FindBall state. This state will conduct a head scan to find the ball, running two sweeps with the bottom camera (one with the head tilted forward, one with the head tilted backward) and two sweeps with the top camera. It will then rotate approximately ninety degrees either clockwise or counterclockwise, depending on information about the ball location transmitted by the goalie, and then repeat these head scans. If the robot detects the ball at any point in this state, it will push FindBall onto its behavior stack and go to the GotoBall state. Furthermore, the robot will constantly perform a role check in this state to determine if it should switch to the support role, in the situation where another robot is preparing to kick the ball.

In the GotoBall state, the robot will move towards the ball, while keeping the ball as close to the center of his vision as possible. Ball-tracking head behavior is alternated with a localization checking behavior, in which the robot glances away from the ball to the position where it thinks a goal should be. This greatly aids the robot in verifying the accuracy of its localization. If the robot loses track of the ball for a long enough period of time, it will pop the GotoBall behavior off of the stack, which will put it back in the FindBall state. If the robot gets within a threshold distance of the ball, it will push GotoBall onto the striker stack and go to the AlignGoal State. The GotoBall state also constantly performs a role check to determine if it should witch to the support role, in the situation where another robot is already closer to the ball.

In the AlignGoal state, the robot will align its orientation such that it is facing a point between the two enemy goal posts. It does this by verifying the enemy goal position with head scanning, and by turning in a circle around the ball until it detects that it is facing the approximate center of the goal. The robot will then push AlignGoal onto its stack and go to AlignKick. Alternatively, if the robot is very close to the enemy goal, it will immediately push to the Dribble state and forgo any alignment. The Dribble state will simply cause the robot to dribble the ball forward for three seconds before popping back to the AlignGoal state. The AlignGoal state also keeps track of the initial time it was activated, so that a timeout system could be used to determine if it should pop and return to the GotoBall state.

The AlignKick state is relatively straightforward. The robot simply moves itself to position its foot relative to the ball so that it can execute a kick effectively. There are, however, multiple aligning states, depending on which kick is executed and which foot is used, so this is where the stack can branch to use different kicks. Once appropriately aligned for a kick, the robot will push the AlignKick state onto the behavior stack, and then go to the appropriate KickBall state, which simply executes a kick motion and pops.

### 3.5.2 Support Role

The support role of the behavior system was designed to allow the robots to play cooperatively as a team, as opposed to individual agents trying individually to complete the same objective. There is an offensive supporter and defensive supporter. The defensive supporter moves towards its own goal area and tries to stop other robots from scoring. The offensive supporter moves towards the enemy goal and is positioned such that if its teammates shoot the ball down the field, it is ready to try to take the ball.

The method for switching between the different roles is decided based upon the current state of the robots and their roles. The robots use wireless communication to transmit what role they are as well as their distance from the ball. If the robot does not receive any communication that indicates that there is an active striker, it will take on the role of a striker. If there are two non-goalie robots, depending on who is closer to the ball, the closer robot will take the role of striker and the farther robot will take on the offensive supporter role. If there are three non-goalie robots active, the closest to the ball will be the striker, the closest robot the enemy goal will take on the offensive supporter role, and the robot closer to its own goal will take on the role of the defensive supporter.

### 3.5.3 Goalie Role

The goalie role is the simplest of the three roles in terms of what the robot actually does. It was designed specifically to keep the goalie in the goal at all times, since due to the rules of the competition a goalie is virtually impossible to be penalized as long as it remains in the goalie box. Keeping the goalie in the goal became even more important once the rules changed to make both goals the same color, since the goalie is now the best indicator of which goal belongs to which team.

The goalie state machine begins in the TrackBall state, where it spends most of its time. As long as the ball is outside of clearing range for the goalie, the robot will simply scan with its head until it sees the ball, and it will then track the ball. This also keeps one robot tracking the ball at all times, and since the goalie's position is effectively constant, it can broadcast a reasonably accurate ball position to all of the other robots on the team. The current Behavior module does not make use of this ball information, but given more time it is a subject that the team would like to explore using more in the future.

If the ball ever comes close enough to the goalie that the goalie can feasibly clear it out of the goalie box, the TrackBall state will be pushed onto the stack and the goalie will move into the AlignBall state. In this state, the robot simply lines up its foot to execute a kick. Once the foot is aligned, AlignBall is pushed onto the stack and the robot moves to the ClearBall state, where the robot executes a kick before popping back to the top of its behavior stack.

## 1.6 Hardware Upgrades

### 1.6.1 New Heads

One of the limiting factors in improving the robots is the limitation of the hardware, particularly the CPU and RAM. Ideally, the robot's software should be able to process the camera images at 30 frames per second at full resolution (640x480). This was not possible with the version 3 Nao robots due

to the processor speed. It was decided that upgrading the Nao heads to the new version 4 hardware would enabled better vision calculations.

Below is a table highlighting the differences in the hardware between the version 3 and version 4 Nao heads.

**Table 1: Hardware Differences Between Nao Version 3 and Version 4**

	Version 3	Version 4
Camera Resolution	640 x 480	1280 x 960
Processor	500 Mhz Geode	1.6 Ghz Atom
RAM	256 kB	512 kB

While there was very little time to test the capabilities of the new hardware, the new hardware was able to compute the saliency scan at quadruple the old resolution while maintaining the required 30 frames per second. This would allow the vision calculations to be more precise at determining the size of small objects such as the soccer ball.

### 1.6.2 Camera Drivers

The biggest change required to get the new hardware to work with the existing software was the camera drivers. The development of a camera module was needed to interface with the ALVideoDeviceProxy to access the camera images on the new hardware. This is in contrast to the old method which used Video4Linux to read the camera images directly from the camera. While the Video4Linux method is the preferred method due to its speed, it was undocumented.

The new camera module was able to read 640 by 480 resolution camera images at 30 frames per second and store these in a shared memory buffer. Initial attempts to read the full 1280 by 960 camera images caused a reduction in frames per second. Particularly, there were some bugs related to using memcpy on the raw camera data which caused the drastic drops in frame rate.

The other issue related to the moving to the new cameras is the camera settings. The new camera had fewer settings than the old camera, which made it more difficult to calibrate the images. Particularly, the color red was not very vibrant which made detecting robots on the red team hard to detect.

### 1.6.3 Build System

Due to the transition to Intel processors, the build system for the warrior software had to be redesigned. The biggest change was to rewrite the 'warriors' script which provides syncing capability with the robots. This was rewritten to address many of the short-comings that the original script contained. The new 'warriors' script allows greater flexibility in specifying which portion of the software should be uploaded to the robot.

### 3.6 Visualization Tool

The visualization tool is a web application for Google's Chrome Web Browser. The application is programmed using JavaScript, HTML, and CSS. It uses some of the latest web technologies such as Web Sockets and WebGL. The features of the visualization tool include:

- Parameterized 3D soccer field with 3D Nao robot models and soccer balls.
- Real-time visualization of robot, ball and goal location.
- WIP: Live feed of robot's raw and calibrated camera images.
- WIP: Supports multiple robots on the field.

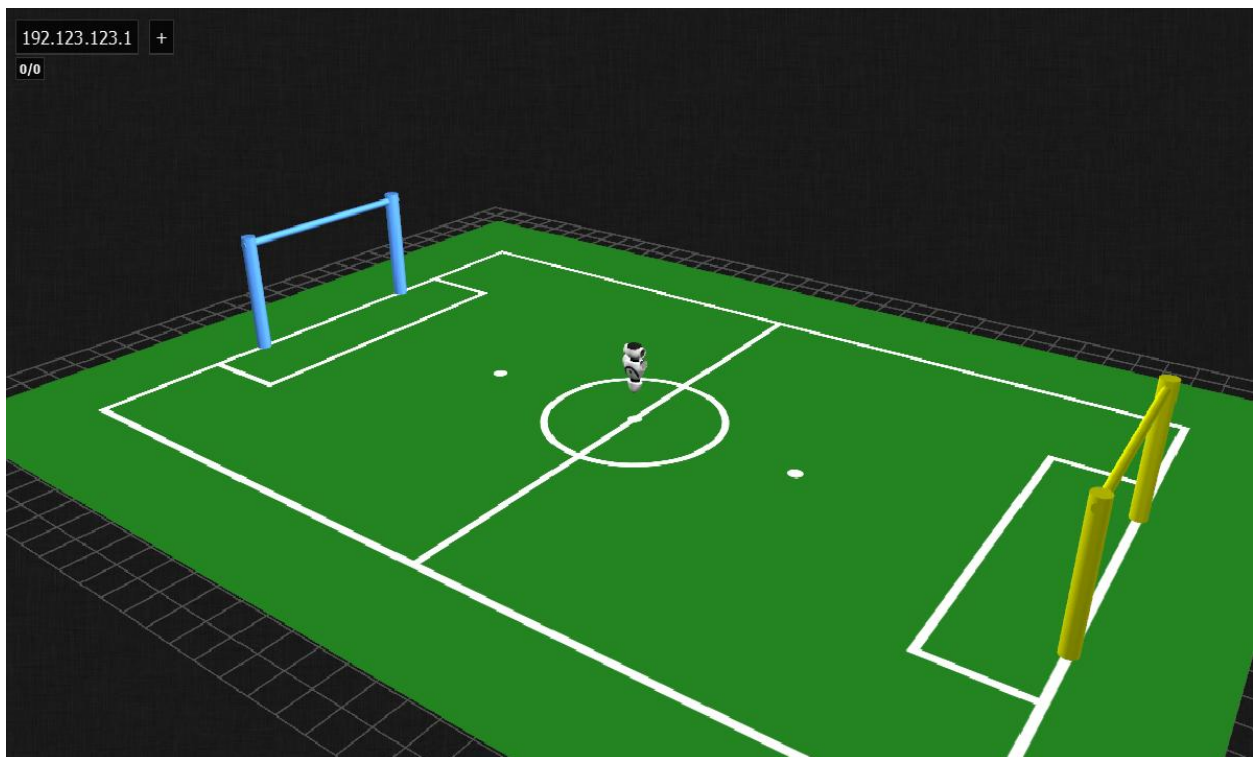


Figure 14: Visualization Tool Screenshot

The goal of the visualization tool is to allow the C++ Warriors application running on the robot to communicate with an external program. The difficult part with this requirement is the fact that web applications cannot use raw TCP or UDP sockets. Modern web standards only allow Web Sockets, which are a specialized protocol layered on top of HTTP. Implementation of the web socket protocol in C++ would be extremely time consuming, so NodeJS was used to bridge the gap.

NodeJS is a server-side JavaScript runtime engine. It has builtin support for TCP, UDP, and Web Socket protocols. This provides the ideal solution to providing communication between the web application and the robot.

The first iteration of the visualization's architecture is shown in the figure below. NodeJS was run on the robot to reduce the latency between the warrior application and NodeJS. It utilized the file system to exchange data with NodeJS which would send the data to the web browser. The advantage of this architecture is the low latency and simplicity. The disadvantage is the need to use valuable processing power on the robot to run NodeJS. While testing showed NodeJS used a small percentage of the CPU, it used a considerable amount of memory.

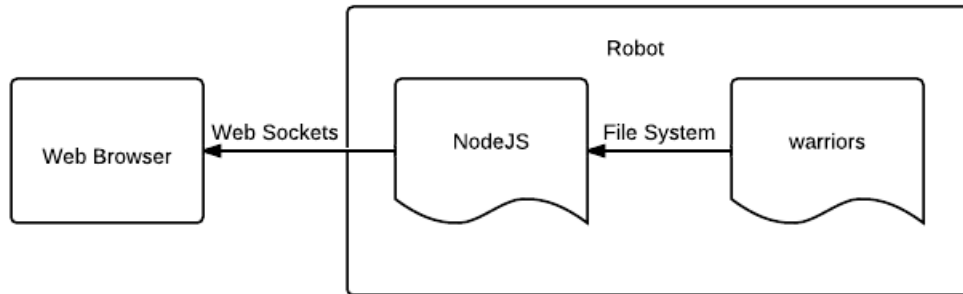


Figure 15: First Architecture of Visualization

In order to stream more data and to reduce the load on the robot, the architecture was changed to remove the need to run NodeJS on the robot. NodeJS can be run on any computer which connects to the robots via UDP sockets. In addition to using less resources on the robot, this architecture allows NodeJS to store lots of image data which is needed when streaming the robot's camera feed.

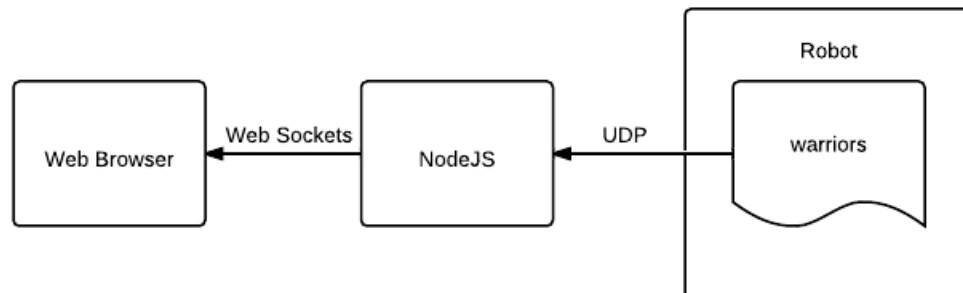


Figure 16: Final Architecture of Visualization

In order to incorporate visualization into the warrior application on the robot, an additional module was added to the perception thread. After vision, localization, and behavior have executed, the visualization module will save all of the data and send out a UDP packet. This is an improvement over the Off-Nao architecture which ran independently of the perception thread. This new architecture guarantees the ability to debug each frame of the perception cycle.

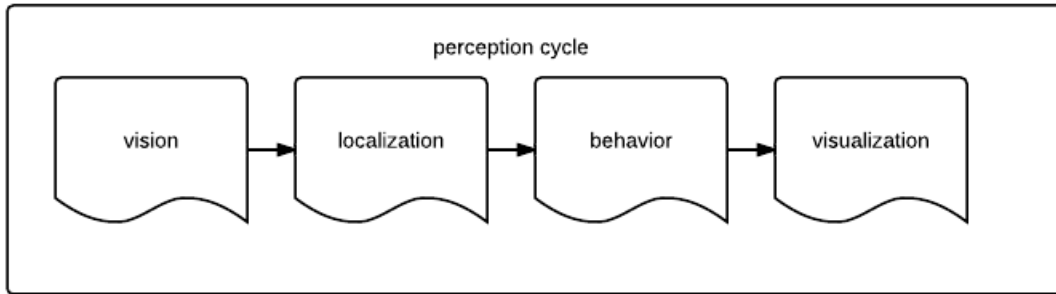


Figure 17: Perception Execution Order

## 4 Results and Discussion

### 4.1 Initial Testing

The initial testing consisted of gathering data on both the vision and localization modules, as well as determining the time the robots took to score on an empty field from various positions. The purpose of the tests was to establish benchmarks to measure the improvement of each module and the overall system by the end of the project, and also to determine what parts of the system needed the most improvement.

#### 4.1.1 Vision

The first module that needed testing was vision. The methodology for the tests consisted of comparing the robot's perceived distances and headings of various objects to the objects' actual distances and headings.

To test the goal posts the robot was placed in one of five different locations and the average reading of the distance and heading to each post was recorded. The placements of the robot are shown in the figure below.



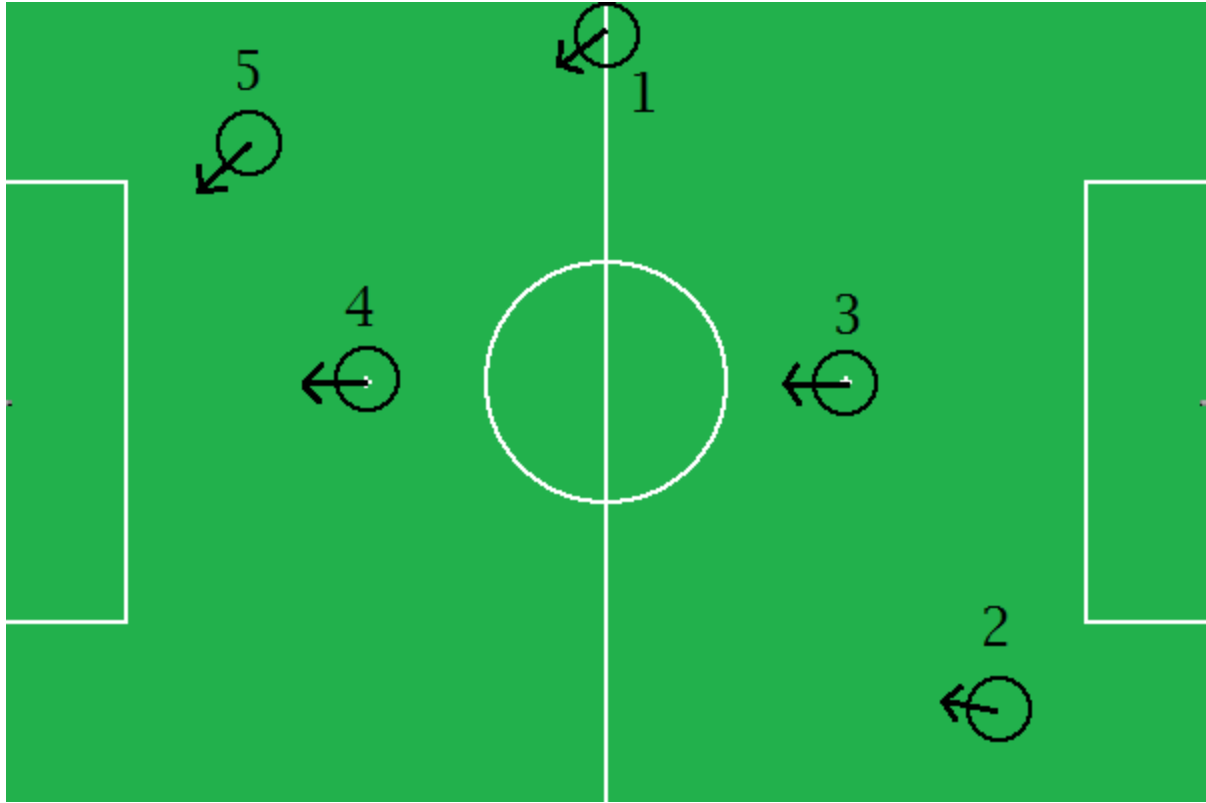


Figure 18: The Five Trials for Robot Placement for Post Vision Testing

The actual distances and headings were then measured to compare to the robot's perceived measurements. The distance to the goal posts is shown in the bar graph below.

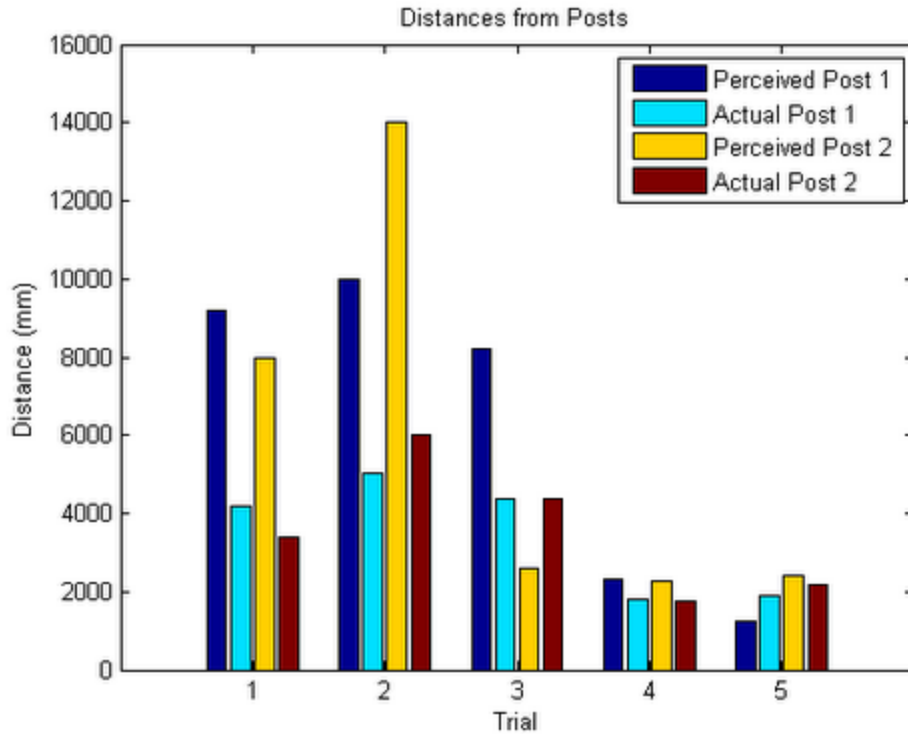


Figure 19: Comparisons of Distances from Posts across All Trials

The trial numbers correlate with the numbers shown on the previously shown field figure. For the trials at or beyond the half-field line, the robot perceived the posts at around twice the actual distance. For the two closer trials (4 and 5) the robot perceived the posts more accurately, in this case within 50% of the actual distances. Overall, the robot perceived the posts as being farther away than they actually were. The only two exceptions were trials 3 and 5. During trial 3 the robot incorrectly lengthened the right post because it saw a few blue pixels on the center circle, far below the actual post. This caused the identified post object to be almost twice as big as it actually was, so the robot determined that that particular post was quite close. Trial 5 was simply an outlier, and the project group is unsure as to why this behavior occurred.

The post heading was significantly more accurate than the post distance. Note that the headings were all quite small, since the robot was positioned facing the goal. The posts were relatively far from the robot, which also contributed to the small headings. The headings are shown in the figure below.

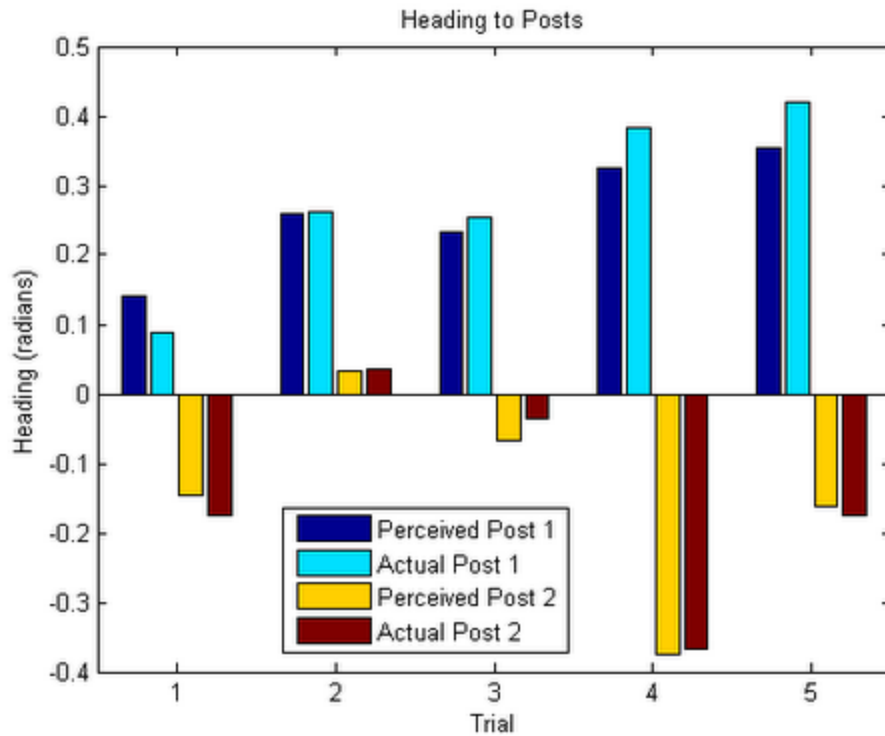
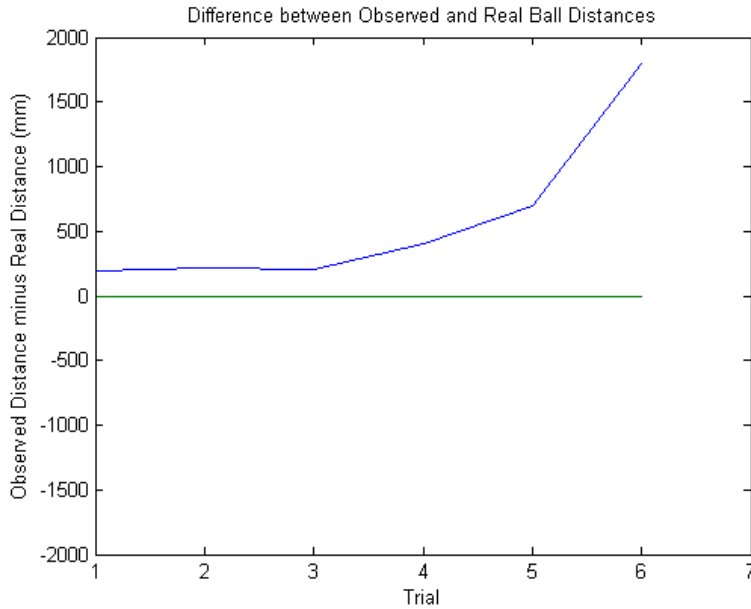


Figure 20: Comparisons of Headings from Posts across All Trials

The error in heading perception was consistent regardless of the distance to the posts. On average the error in heading perception was about 0.02 radians. Unlike with the distances, there is not much to improve on in determining the heading.

The ball distance showed a similar trend to the post distance, which was to be expected since similar algorithms calculated both distances. The data is shown in the plot below.



**Figure 21: Difference between Observed and Real Ball Distance**

The trials were conducted over a variety of distances: 500 mm, 1000 mm, 1500 mm, 2000 mm, 3000 mm, and 4000 mm. For trial 6 the robot did not perceive the ball at all. The error in ball distance increased the further away the ball was.

#### 4.1.2 Odometry

The second module to test was the odometry. The robot can move in three directions—directly forward and backward, strafing side to side, and turning about its center (denoted forward, left, and turn respectively)—and each motion has its own odometry function for computing the expected change in position and orientation. The tests had two goals: to measure the overall error of the system for each motion and to determine how consistent that error was over many trials and different distances. In theory the error should follow a linear function, because odometry updates occur over short periods of time, and the error should propagate depending on the duration of the tests. Due to issues with the motor and the carpet, however, this was not always the case.

The forward tests were conducted by starting the robot at a specific starting point. The robot then walked forward until the odometry calculated that it had reached its target, and this test was repeated over six trials. The targets ranged from 250 mm to 1500 mm, increasing at increments of 250 mm. The actual distance travelled was recorded for each trial, and error was calculated by subtracting the expected measurement (the target odometry reading) from the actual distance. The results are shown in the figure below.

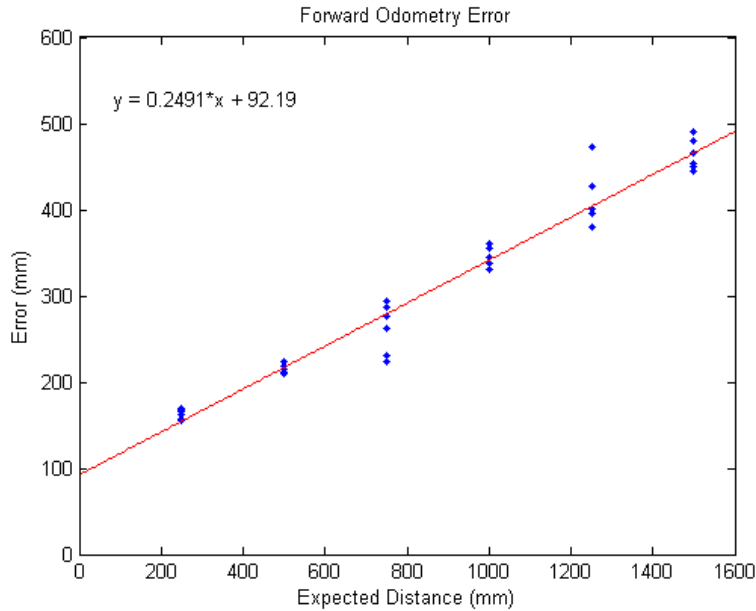


**Figure 22: Expected Forward Distance vs. Error**

The overall error was quite consistent. The forward odometry always underestimated the distance walked by the robot, and the underestimation closely followed a linear function. The error was also consistent for each expected distance, with the largest difference in the data points being approximately 100 mm when the robot traveled 1250 mm. This data shows that the forward walking motion is easily predictable, and therefore the forward odometry could be made more accurate with a simple software correction. The correction itself would vary from robot to robot, but each adjustment could easily be calculated by repeating this experiment for each robot.

The left odometry tests were conducted in the same manner as the forward odometry tests, except that the robot was placed sideways on the field and strafed left until it reached its target. Also, the targets in this case ranged from 150 mm to 900 mm over 150 mm increments, because the robots do not strafe nearly as far as they walk forward (with the exception of the goalie, who at most needs to cover the relatively small area in front of the goal posts). Again, error was calculated by subtracting the expected distance from the actual distance travelled.

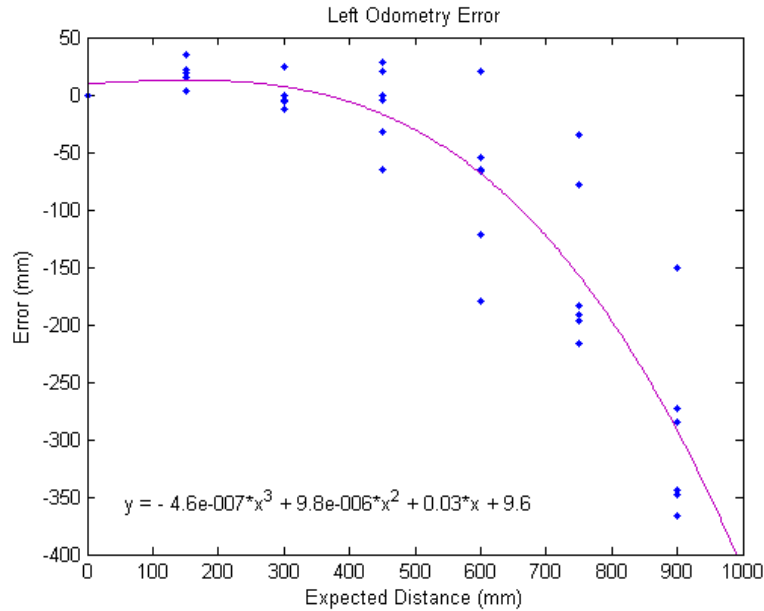


**Figure 23: Expected Left Distance vs. Error**

The results were much less consistent than the forward odometry results. The data points were much more spread out as the distance traveled increased beyond 300 mm. At its worst, the data varied by 225 mm at a distance of 900 mm traveled. However, the error was actually quite low (within a few mm of the actual distance traveled) over short distances. This behavior resulted in a cubic function fitting the data best, even though the data should have linearly added up as the error propagated over long distances. This was probably due to the often observed fact that the left walking motion is prone to more interference from bumps in the field surface and leg motors overheating. Also of note is that, unlike the forward odometry, the left odometry overestimates the distance traveled. The robot's actual distance traveled consistently failed to reach the target over longer distances.

To attempt a software correction for the left odometry, a linear fit is required. The best linear fit of the data is shown in the figure below.

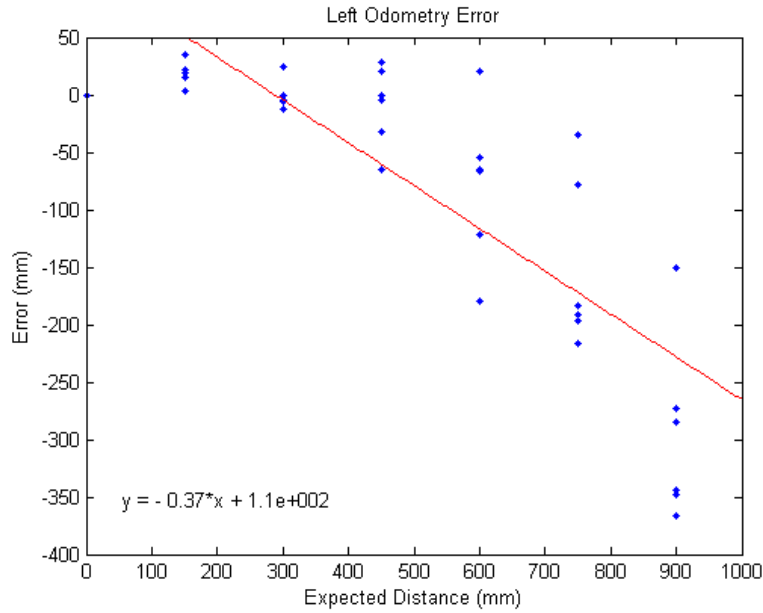


Figure 24: Linear Fit of Left Odometry Error

While using this function as a software correction for the error could improve the odometry a bit, the data is too unpredictable for this to be a good solution. These results suggest a more in-depth solution, such as improving the consistency of the strafing motion itself.

The turn odometry test used the same six trial method as the previous two tests. The robot was started at an initial orientation and turned until it reached its target orientation, with targets ranging from 30 degrees to 180 degrees at 30 degree increments.

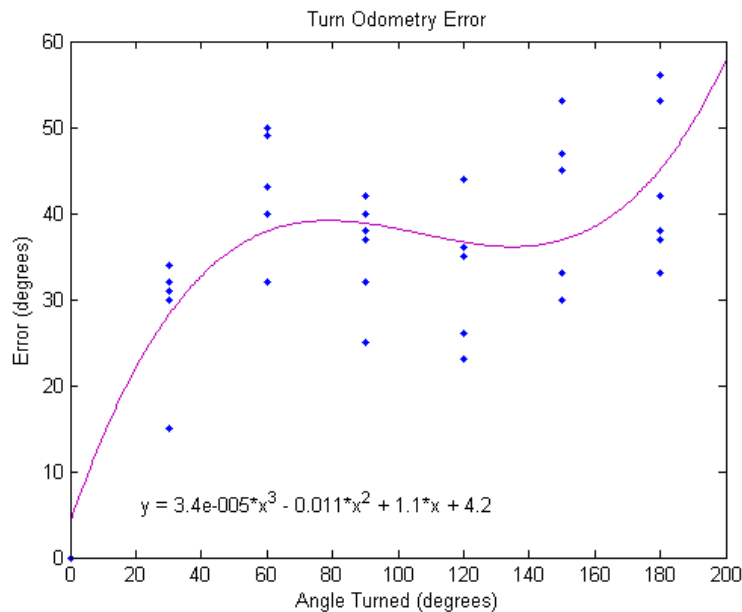


Figure 25: Expected Turn Angle vs. Error

This data was also best fit by a cubic function because again, it was very inconsistent. The actual angle turned varied widely at any target angle. Since the turning motion has similar problems with carpet interference as the strafing motion, similarly inconsistent odometry results were expected.

As with the other tests, linear regression was applied to the data points to see if a software correction could minimize the odometry error.

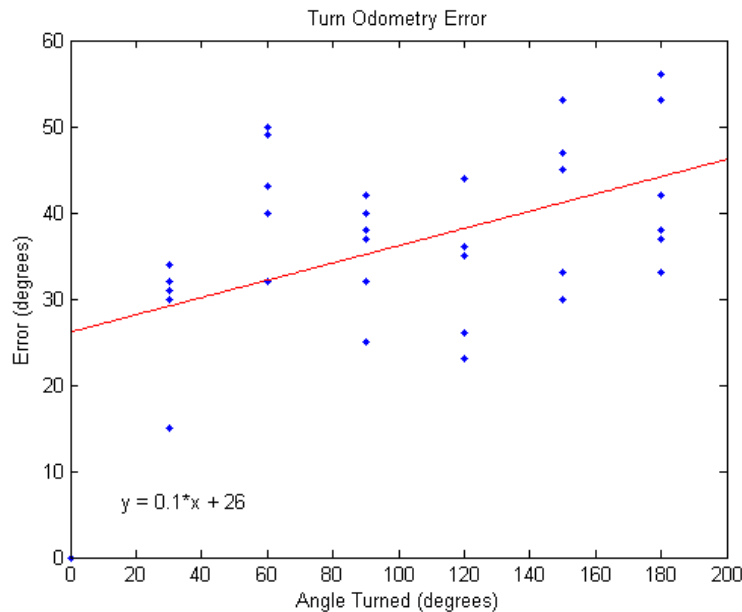


Figure 26: Linear Fit of Turn Odometry Error

Again, this fit is not very good. The linear function could be applied at each odometry step (probably with more success than for the left odometry, since the turn odometry is at least consistent in that it underestimates the data for all distances), but there is still too much spread in the error for this to be a good solution. Improving the turning motion itself would be the best way to fix this error.

### 4.1.3 Localization

The third module that needed testing was localization. These tests incorporated both the vision and odometry data, so they were somewhat dependent on the accuracies of both, detailed in the preceding two sections.

The robot's localization module is based primarily on identifying goal post features from the vision data. Failing that, the robot bases its localization on odometry data until another goal post comes into view. In theory, the error for this absolute position should be dependent on field feature detection accuracy, as well as the odometry error. Based on the accuracy of the vision data compared to the odometry data, there should be a dip in error once a feature is detected, and increases in error when the odometry is being used for long periods of time.



In order to properly test the interaction of these factors, the robots operated under normal game conditions for a period of time. The graphs consisted of actual positions and orientations of the robot versus the robot's expected pose from the localization algorithms. This data consisted of the x position, y position, and the heading of the robot. The starting positions were randomized to account for different situations. The first trial was conducted with a sub-optimal calibration, to observe how well the robot localized based mostly on odometry. The second trial represented a normal situation where the robot started looking away from major field features, such as the goals. The third trial also represented a normal situation, except the robot started facing a goal. The fourth and final trial simulated the situation where the robot is penalized, and therefore "kidnapped" from its original position.

The first trial's data is shown in Figure 6 below. The graph on the left shows the trajectory of the robot, with the actual trajectory in red and the robot's estimated trajectory (as calculated by the localization) in blue. The graph on the right shows the overall error as a percentage of the maximum possible error for each variable.

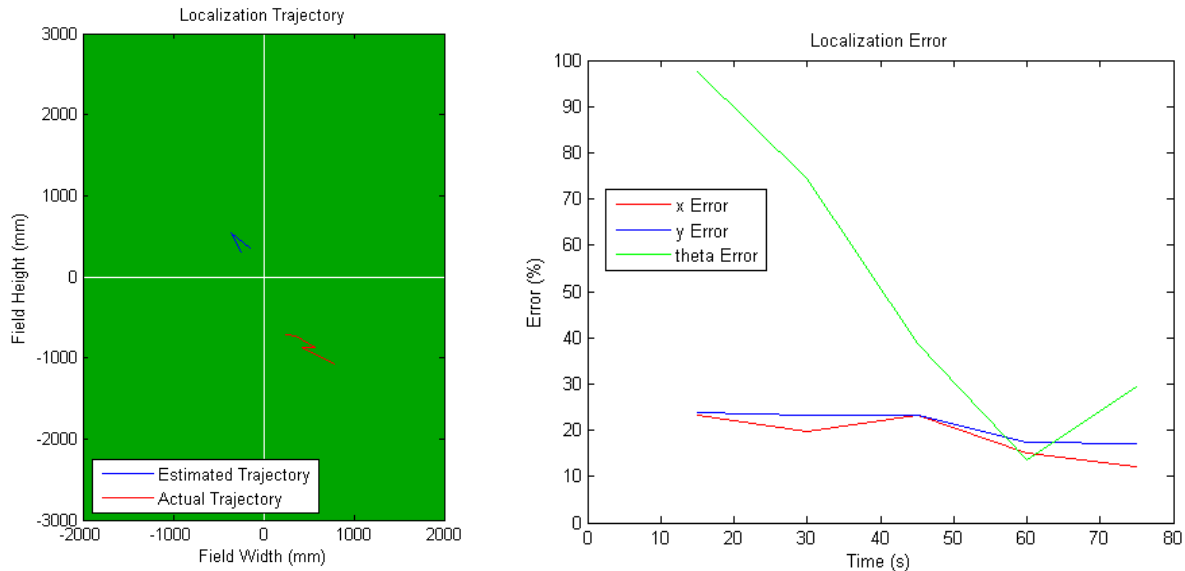
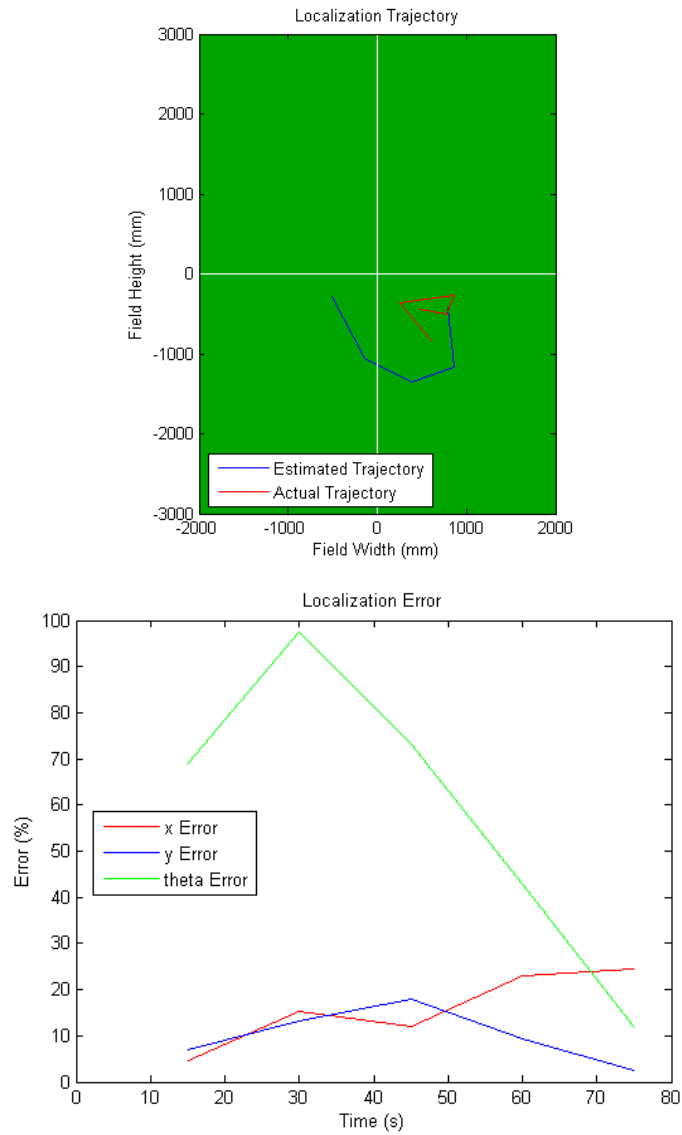


Figure 27: Trial 1 Trajectories and Error

The robot believed it was in a completely different quadrant of the field for this trial. The distance traveled is relatively close; however the headings and positions were completely different. The theta error slowly improved, as did the x and y position data. Theta was the worst of the parameters—this is likely due to the algorithm's exclusive use of goals as reference points—if there is no goal, then erroneous odometry alone determines position. Data from trial 2 showed a similar trend in regards to theta error.



**Figure 28: Trial 2 Trajectories and Error**

The trajectories were closer, possibly due to better calibration values being used. The errors show more clearly the effects of odometry error. The largely incorrect theta value caused the robot to believe it was moving in a different direction. However, the error improved toward the end of the trial as the robot faced one of the goals, correcting the odometry error.

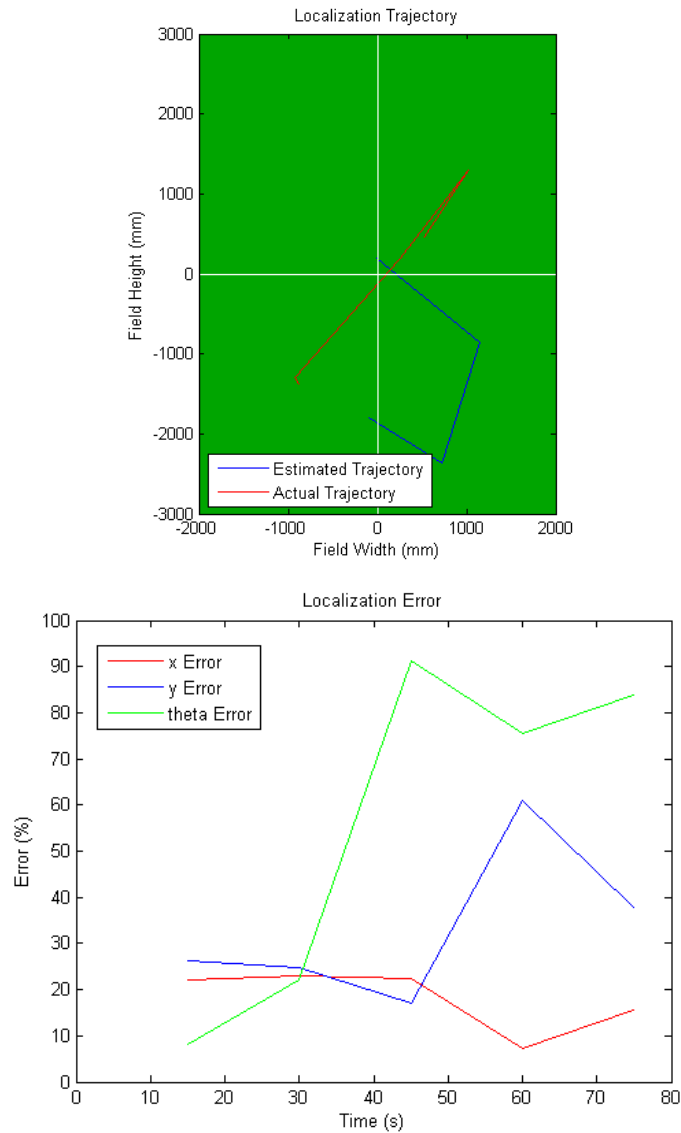


**Figure 29: Trial 3 Trajectories and Error**

The trajectories of the third trial started off with a relatively small error, but that error increased significantly as time passed. The theta error started off small, but increased over time—trial 3 is the only time where this is the case. This behavior was expected, since the robot started by facing a goal. The initial reading was relatively accurate, but as soon as the robot chased after the ball, odometry took over and the error propagated. Additionally, while x error decreased over time, y error did not, instead spiking in the middle of the trial. This could be either because of odometry error or false landmarks.

The last trial included a scenario where the robot was “kidnapped” (which occurred between the first and second data point), or repositioned as if it had a penalty. There is no odometry data available for such a scenario, as the robot is physically picked up from the field, and put down somewhere else. The expected result of this situation would be a sudden spike in error.

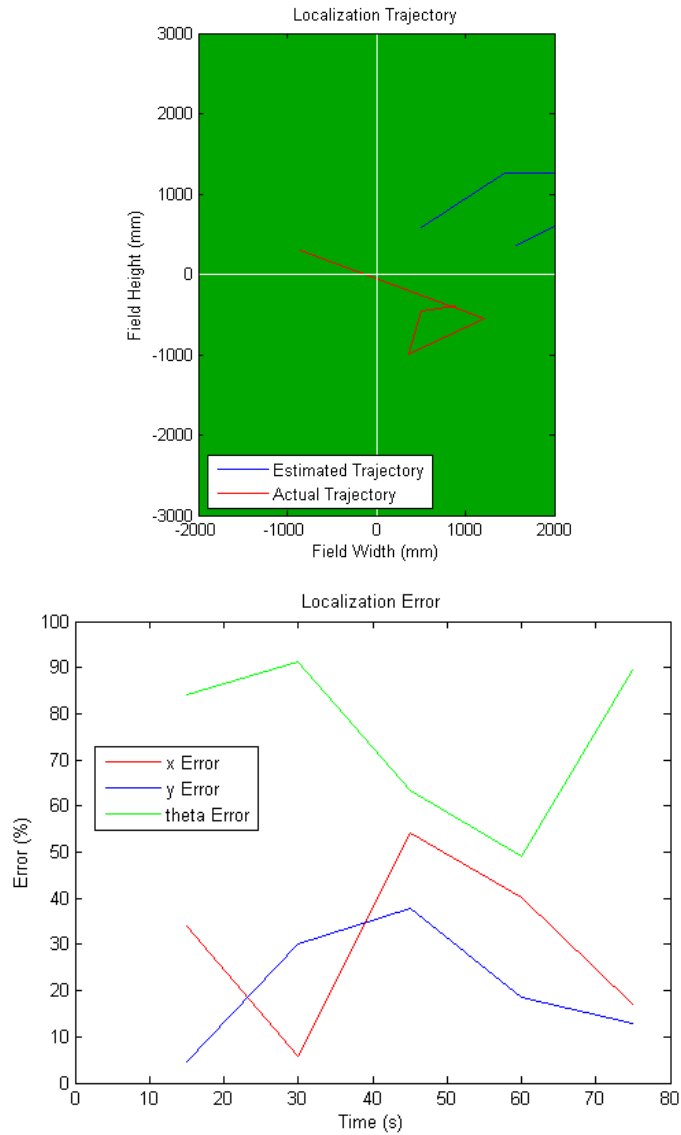


**Figure 30: Trial 4 Trajectories and Error**

The error shows that the robot did suffer an increase in error due to the kidnapping—except in the case of x. This could be due to the robot seeing a feature whose position was much more accurately determined in the x direction, but this is unlikely because the theta error and the y error both increased. If a feature was seen, the y and theta error should have improved somewhat as well. Another possible, and more likely, explanation is that the kidnapping improved the x value by pure luck.

To determine overall pattern of x error across the four trials, a plot of all x errors is displayed below.

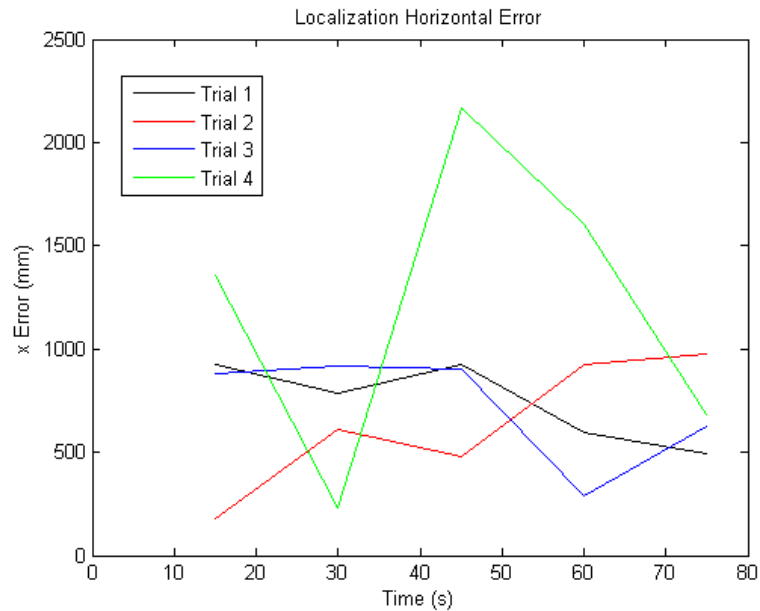


Figure 31: Overall X Error Data

The x error was relatively consistent, staying below a meter until the last trial. The errors each follow a pattern of increasing over time, until a feature is spotted. The last trial was the trial where the robot was kidnapped, which would invalidate odometry until a feature was spotted, which would allow the robot to re-ascertain its position from a known point of reference. The best way to fix the consistent x error of about a meter would be to correct odometry errors. Correcting the vision would also improve the error, but less so than the odometry.

On the surface, the y error appears to be different than the x error. However, the trend is actually quite similar to the x error. The field is 50% longer in length than in width, and the average y error is about 50% greater than the x error, as shown in the plot below.

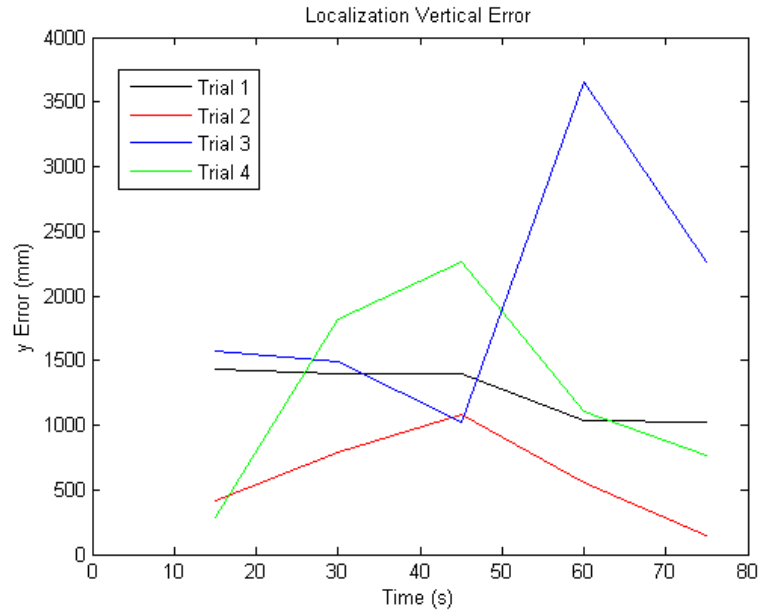


Figure 32: Overall Y Error Data

The y error was more severe than the x error, running at about a meter and a half on average. When paired with the data regarding the x error, there is interesting behavior, in that they do not always parallel each other. This indicates that odometry has an axis-specific error, or that feature recognition is better for different axes based on the position and orientation of the robot.

The final distinct variable observed was robot heading, recorded in the figure below.

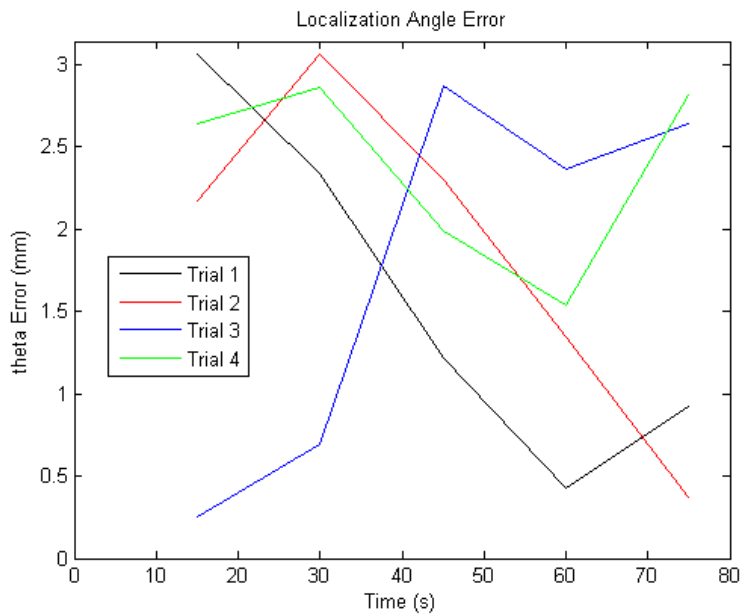


Figure 33: Overall Theta Error Data

The theta error showed rather consistent trends. In trial 3, the robot was started in front of a goal, while in all other trials, it was not. When started without an immediate feature reference such as the goal, the error steadily decreased, while in the opposite situation, the error started low and increased. The increase very clearly demonstrates the error in odometry—error increases due to the absence of known reference points, as the odometry error propagates. The decrease in error in other trials is likely due to the sighting of a goal, and the steady integration of that data as it is confirmed by multiple sightings. The best way to fix this error would be to improve the algorithms governing the calculation of initial position, and to correct the odometry errors.

#### 4.1.4 Time to Score

As a final benchmark test, the project group measured the amount of time it took a single robot to score a goal on an empty field. The robot started in the middle of the center circle for each test, with the ball position varying for each test. The ball was placed on the edge of the center circle, on the left side of the field between the “+” field marker and the sideline, on the left side of the field between the “+” field marker and the sideline, and centered on the goalie box. These four positions were repeated on both sides of the field, for short- and long-distance testing.

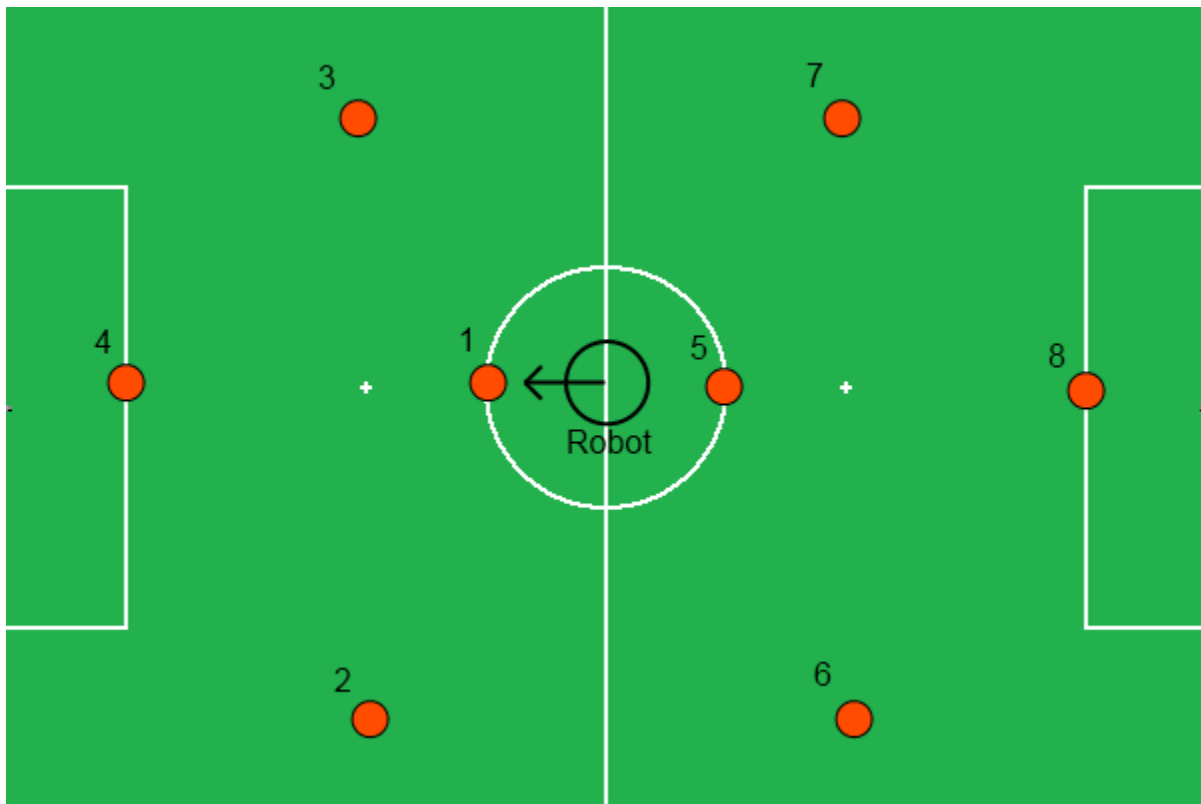


Figure 34: Robot Initial Position and Ball Positions for Time to Score Tests

Each of the eight trials was run until the robot scored. Some trials took multiple attempts, as the robot would either kick the ball into what the project group judged was a stuck position (e.g. the ball resting against the outside of a goal post), or a combination of motor overheating and carpet imperfection caused the robot to be unable to turn properly. The robot would eventually score in many of these

cases, but the times would be misleadingly high, as this test was not a test of motor malfunctioning or terrain defects. As a result, the times kept for each trial represent a “best” time to score, i.e. a time where the robot did not encounter an unexpected problem. The times were as follows:

**Table 2: Time to Score from Varying Ball Positions**

<b>Trial</b>	<b>Best Time to Score</b> <i>min:sec</i>
1	0:40
2	1:23
3	2:02
4	0:30
5	2:07
6	4:12
7	2:44
8	4:15

As expected, all of the half-field trials (trials one through four) resulted in faster scoring times than the full field trials (trials five through 8), since the overall distances were shorter, and the robot did not have to turn around and walk away from the goal to get to the ball. Both trials where the robot, the ball, and the goal were directly in line (trials one and four) took a relatively short amount of time for the robot to score. If the ball was placed on the side of the field, however, the robot took significantly longer to succeed, since the robot had to make more turns and cover more distance to get to the ball and align itself with the goal. Approaching the ball on the right side of the field was particularly difficult for the robot, as shown by trial three, because the scanning pattern for the ball involves the robot turning counter-clockwise, which has the robot scan the left side of the field before the right.

All four of the full field trials took between two and five minutes to score. These times are harder to draw any conclusions from, because over the much greater distances that the robot had to cover, more issues could occur between when the robot first reached the ball and when the robot finally scored.

## **4.2 Final Testing and Individual Module Discussion**

At the end of the project, the team revisited the initial tests to determine how much each module was improved. Vision, odometry, localization, and time to score were each tested using the new software modules. An analysis of the results of those tests is shown below.

### **4.2.1 Vision**

The team continued to perform testing on the vision module as the software and hardware changed. The first of these tests measured goal post and ball distance accuracy with the modified software and the old hardware. Another set of tests analyzed the effect of the new high-definition cameras on the accuracy of the vision module.



### 4.2.1: Final Post Distance Testing

The team performed the final testing of the vision module using the same method as that in the initial testing, as described in the Vision section of the Methodology.

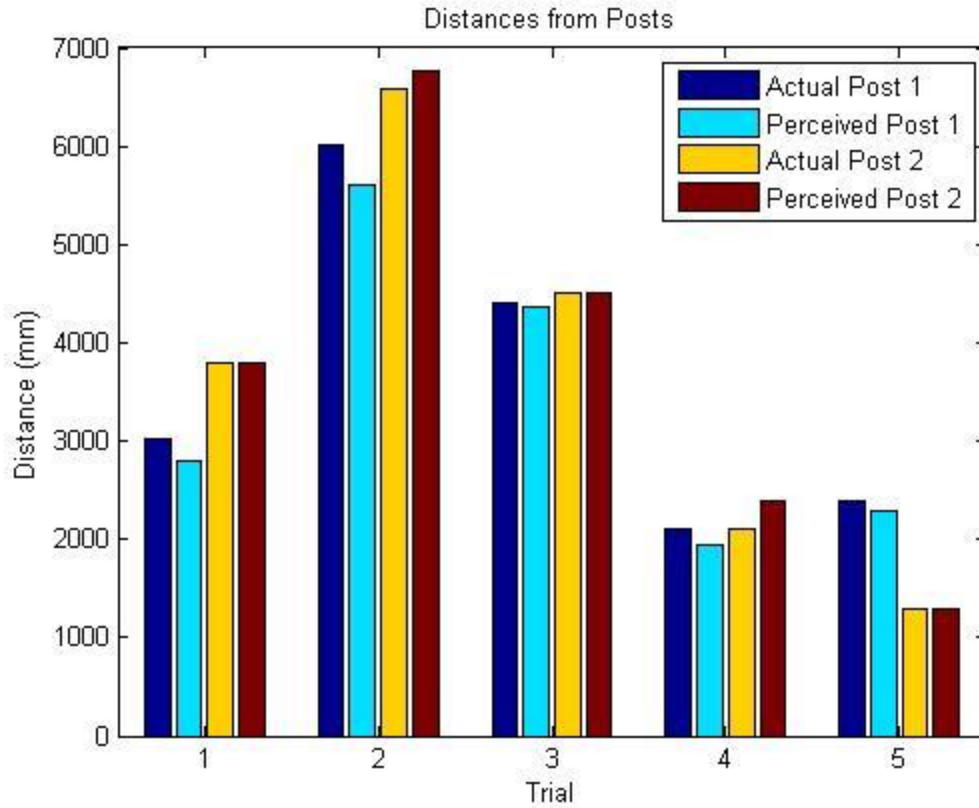


Figure 35: Comparisons of Distances from Posts at Various Positions After Software Changes

As can be observed from the graph above, the results from the distance measurements show great accuracy. Every perceived post distance is close to its respective real post distance. The results are much more accurate than those measured in the initial testing. This increase in accuracy is most noticeable for farther distance measurements, where the error was particularly large in the initial test.

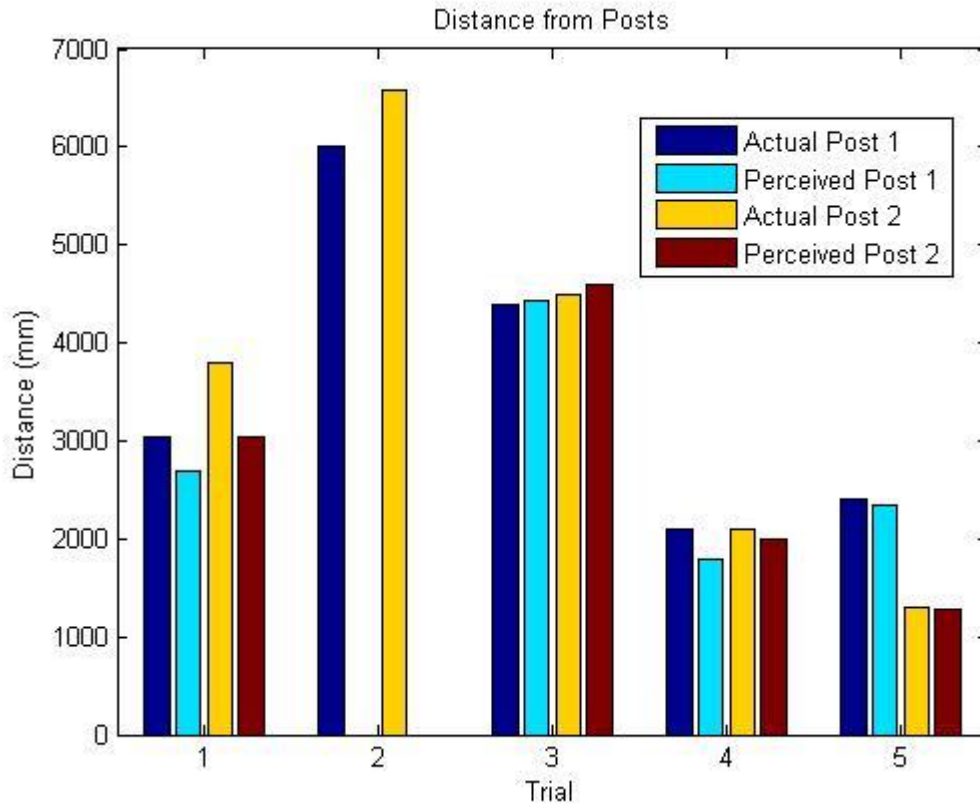


Figure 36: Comparisons of Distances from Posts at Various Positions after Hardware Changes

As opposed to increasing the accuracy of post distance measurements, the new hardware actually caused a slight increase in the error. Furthermore, during the testing, some posts did not get seen at all, specifically during trial 2, where the posts were the furthest away from the robot. Even with this decrease in accuracy, the results are still dramatically more accurate than the results acquired during the initial testing phase.

#### 4.2.2: Final Ball Distance Testing:

The team applied the same methodology for the ball distance calculations.

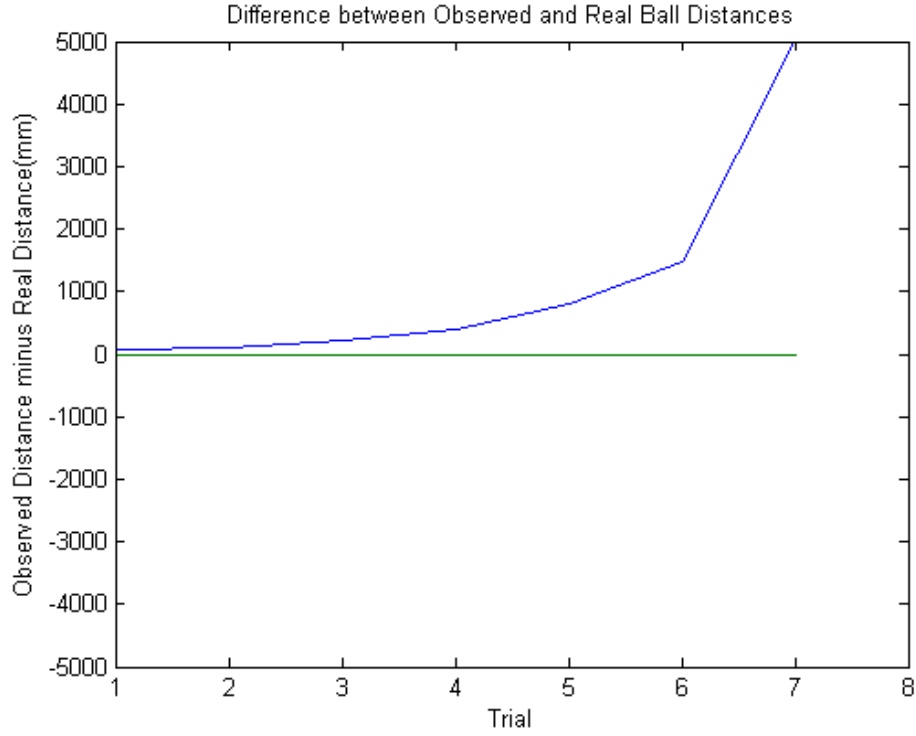


Figure 37: Difference between Observed and Real Ball Distance after Software Changes

The error shown in the graph above is very similar to the error found in the initial test. This is due to the fact that very little changes were implemented that affected the ball distance calculation algorithms.

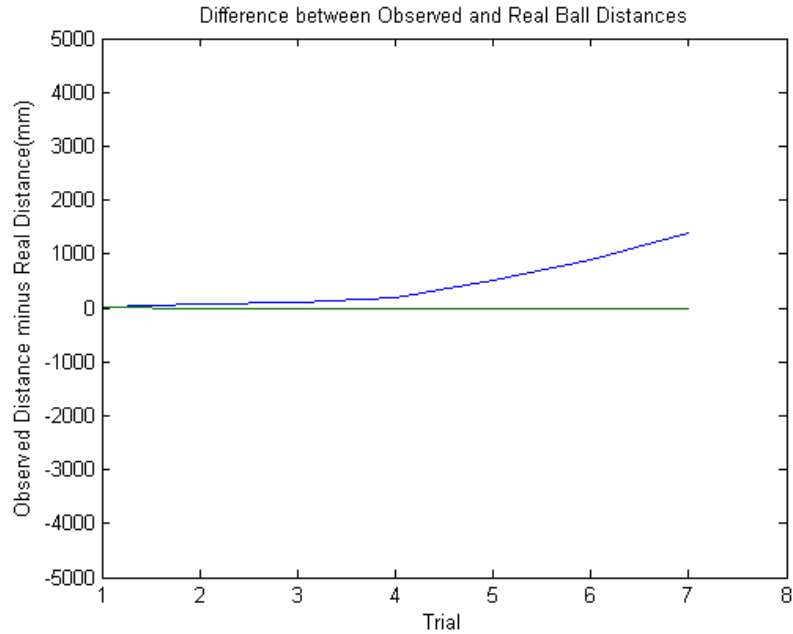


Figure 38: Difference between Observed and Real Ball Distance after Hardware Changes

This graph demonstrates the ball distance error using the new hardware, which provides a higher resolution camera, as well as more processing power. This power allows for the processing of larger images, which is particularly important for calculating the distances of small objects such as balls.

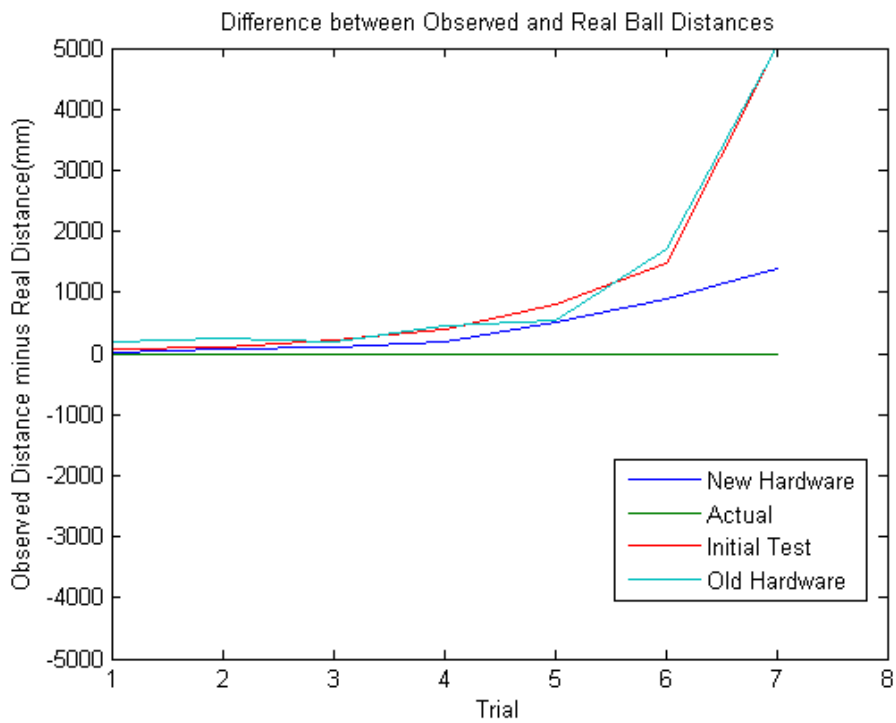


Figure 39: Comparison of Differences between Observed Ball Distances for all Tests

As the graph above demonstrates, the new hardware greatly decreased the error in calculating the ball distance. The decrease in error is particularly noticeable at long distances, where the error with the new hardware was only a third as high as that with the old one.

#### 4.2.2 Odometry

After implementing a system to calibrate linear corrections for the robots' odometry, the same odometry tests were run again to determine the level of improvement. For this iteration of tests, only three data points were gathered at each target distance. As the initial tests show, the distances that the robot moves have little spread, so it was not necessary to collect six data points at each distance.

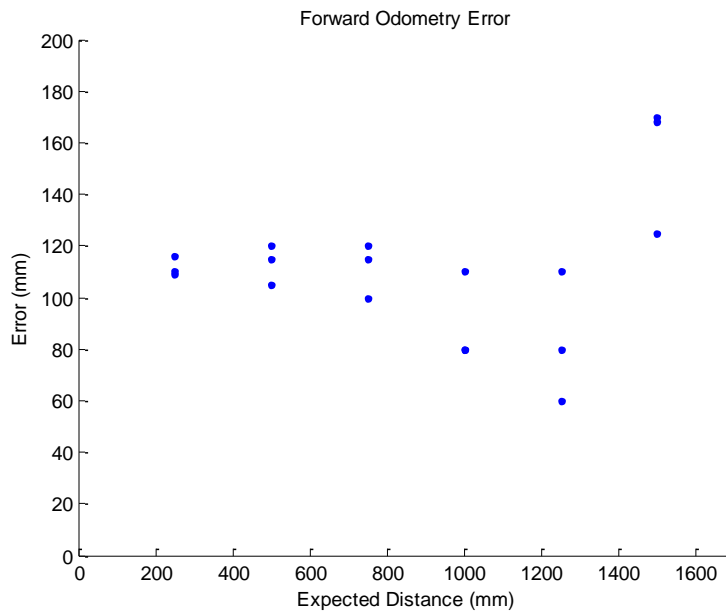


Figure 40: Expected Forward Distance vs. Error

The forward odometry data shows considerable improvement from the initial tests. The error stays around 115 mm, where previously it averaged around 300 mm, peaking at 500 mm. The linear correction significantly improved the robot's forward odometry, reducing the error by 62%.

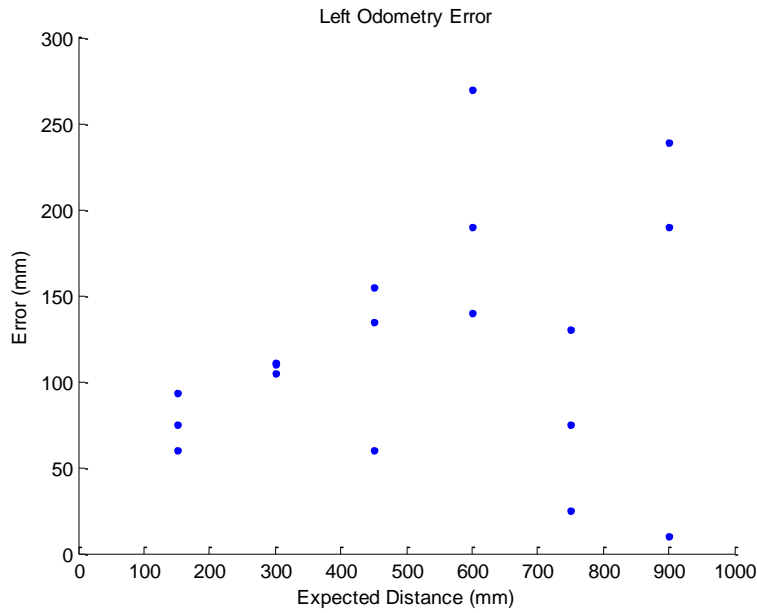


Figure 41: Expected Left Distance vs. Error

Similar results can be seen for the left odometry. Initially, the error averaged around 200 mm, peaking at 350 mm. With the linear odometry correction in place, the left error averaged around 125 mm, peaking at 275 mm. Left odometry error was reduced in this case by 38%.

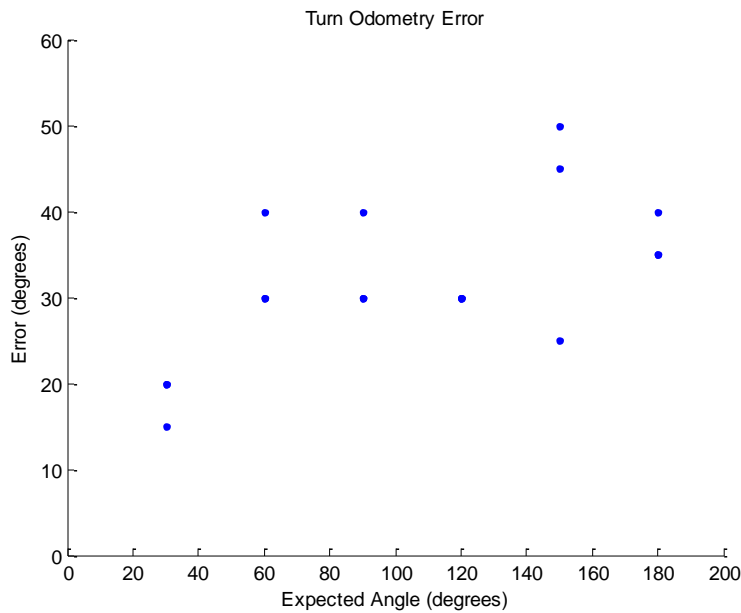


Figure 42: Expected Turn Angle vs. Error

The turn odometry results are about the same as in the initial odometry tests. Both average around 35 degrees. The data still loosely follows a linear trend, however, so with more calibration it is possible that this error could be reduced.

Overall, the linear odometry corrections were successful. Error was significantly reduced in almost all cases. Furthermore, more time spent calibrating could lower the error even more. Improving the correctness of the odometry can greatly improve the accuracy of the localization module, since odometry is one of the two major inputs to the module.

### 4.2.3 Localization

Tests similar to the initial localization tests were carried out with the new localization module. The results are shown below, organized by which filter the localization module was running. All final localization tests were run after the 2012 rule switch, which changed the two goal colors to a single color.

#### 4.2.3.1 Particle Filter

The particle filter system was completed as designed, but several unforeseen issues caused delays in its implementation and testing. Furthermore, hardware limitations prevented the traditionally use of a large number of particle – particle filters usually use particles on the order of hundreds or thousands, whereas our implementation used one hundred and twenty. Despite this, when provided with accurate sensor data, the particle filter was able to successfully determine the robot's location on the field.

The particle filter implementation for this project was determined to be too inaccurate for constant use during the Robocup competition. Though the filter operated as intended, sensor inaccuracies and limitations in processor power and available memory made reaping the benefits the particle filter method offers over the Kalman filter method extremely difficult. This determination was made based off tests conducted on a full field setup in the lab.

The main hurdle to using the particle filter was the hardware available. A particle filter's performance is largely based on the number of particles which it can track. Initially, the onboard memory could only support sixty particles, which was increased to one hundred twenty by redesigning the data structure which holds the particle data. Further increases in the number of particles were prevented due to the amount of time required to perform calculations on the entire set of particles, which increased by an exponential degree as the number of particles was increased.

Another hurdle to the use of the particle filter was the variability and frequency of data provided. As goal posts were the primary landmark used to determine position, when the vision system did not detect a post, the particle filter was severely hampered in its ability to increase the accuracy of the robot's position. Additionally, it was extremely difficult to detect robots on the field in certain lighting conditions, which eliminated the primary method for determining which end of the field is being viewed for a large percentage of the localization routine iterations.

In addition to issues with the filter itself, there were issues with the ability to efficiently test potential solutions to software issues. The methods used to download code to the platform prevent use of traditional debuggers, and compiling and running tests on the platform is time consuming. Additionally, running tests directly on the platform can provide misleading results, as there are a multitude of other systems causing variability in the test environment, which is not desirable for an

initial test environment. These problems were addressed by creating a test setup with a simulated robot and program framework, allowing isolation and debugging of specific particle filter operations.

Aside from this, the filter performed well, especially taking into account the limitations placed upon it. The filter could accurately determine the robot's position given accurate sensor data in a short amount of time. It correctly eliminated and replaced low probability particles in a way which increased the overall accuracy of the predicted position over time. Further, the filter accounted for odometry data and was designed in a way to be extensible should other landmarks be made available from vision to localize off of.

There are several ways to improve the performance of the particle filter system from its current state. The highest positive impact on the filter's performance would be gained by finding a way to significantly increase the number of particles used by the filter. This could be done by finding ways to perform operations on multiple array indices at once (technology which is already used in GPUs), and finding ways to reduce the number of times the array of particles is iterated over each localization routine iteration.

Another way to improve the performance of the filter would be to pre-process the provided data more extensively. One option for this is to check the variability of consecutive post distance and heading readings, and to evaluate how accurate the odometry readings are based on the particle filter's position data, fusing those values using a weighting system.

Additionally, the algorithm to determine the boundaries within which new particles are generated could be improved. Currently, the algorithm evaluates the density of particles within an area and picks the highest value. Instead, each particle could be surrounded by a box of a standard size. Overlapping boxes could be combined, until all remaining boxes are completely separate. The two boxes whose contained particles had the highest average probability would be selected for use, and new particles would be generated within them. This algorithm is potentially more efficient and more accurate in determining particle regions, which would lead to better performance and better run times.

#### ***4.2.3.2 Kalman Filter***

Results of testing the Kalman Filter were generally favorable compared to the old localization module. As with the previous tests, the robot ran its behavior code under game conditions while localization data was gathered. Below is a comparison of the robot's estimated trajectory and the robot's actual trajectory.



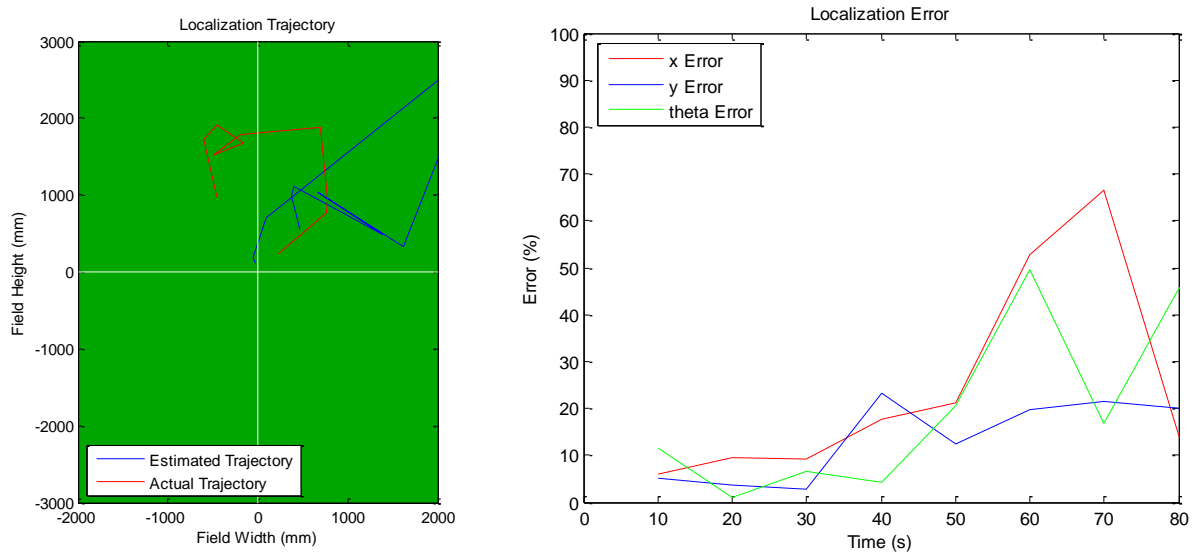


Figure 43: Kalman Filter Trajectories and Error

The trajectories alone may initially seem to be quite erroneous, but when the error is taken into account it shows that the position is not as bad as it looks. The jump to the right of the estimated trajectory is only a single jump in error, and the robot actually managed to correct this error as the test continued. Looking at the graphs of error percentages, it remains low throughout most of the test for x, y, and theta. The error propagated a bit as the test went on, but this is to be expected with a Kalman filter, and as the robot saw more goals, the error was corrected.

After the rule change made both team's goals the same color, another test was devised for the localization module. The robot was placed on the field with a goalie in each goal, and allowed to kick the ball around until it scored in one of the goals. After performing this test multiple times, the robot consistently scored in the enemy goal. There were situations where the robot would kick the ball towards its own goal, but once it got close, the localization module corrected its position and it returned to aiming at the enemy goal.

Between these two tests it is clear that the Kalman filter localization is a significant improvement on the original localization module. Error was lower overall, and the robot was able to recover from error given enough time. More importantly, the new localization was sufficient to prevent the robot from scoring on its own goal, whereas the original localization was not consistent enough to handle the same color goal case.

The biggest issue with the Kalman filter is that it does not handle the case of penalization when a robot is "kidnapped." Since it requires an accurate previous position to run effectively, being picked up and moved messes up the calculations significantly. The robot can eventually re-localize, but it takes some time due to the smoothing effects of the Kalman filter algorithm. This could be improved somewhat by using communication with other robots to determine which side of the field the robot is entering after penalization. Further improvements to the general algorithm could be made by localizing

based off of the white field lines on the soccer field instead of using only the goal posts and the field edges.

#### **4.2.3.3 Complete Localization System**

The original plan for the localization system was to switch between the Kalman and particle filters. However, this proved to be untenable, as the particle filter was unable to perform to the required level on the hardware available. The particle filter ran slowly due to the number of particles it has to maintain, and its accuracy and speed of improvement were limited due to the issues with the number of particles that could be tracked at one time. The final setup of the system was to use the Kalman filter with a relatively accurate estimated initial position. This took some burden off the processors, and was accurate enough for the purposes of the project.

The problems of the Kalman filter, specifically the inability to localize quickly after penalization, did become more apparent once the particle filter was dropped. The particle filter was specifically implemented to handle this case, so as only the Kalman filter was used, the localization system as a whole was not optimal. The biggest improvement to the localization module as a whole would be realizing the successful implementation of particle and Kalman filter switching.

#### **4.2.4 Time to Score**

Repeating the time to score tests with the new code proved difficult. With the change in the game rules resulting in two goals of the same color, comparisons to the old time to score tests do not necessarily make sense. Furthermore, due to bugs introduced by the new robot heads, the results were highly inconsistent.

Running the half-field time to score tests produced equivalent times for the robot to score provided that the ball was directly in line with the goal. However, whenever the ball was placed on the sides of the field, unsolved vision bugs caused by the new heads prevented the robot from scoring in a reasonable time frame.

Theoretically, the times should have been improved, and the original bias for scoring on the left side of the field faster than the right should have been eliminated. This is because the new behavior code, in conjunction with the new localization code, was specifically written to allow the robot to turn in the optimal direction at any point on the field. Subjective evaluation of a robot's turn direction decisions showed that the robot turned in the correct direction most of the time, from many different locations on the field. Due to the bugs with the new heads, a more objective evaluation of improvements on the robot's time to score was unable to be conducted.

### **4.3 Discussion of the System Performance as a Whole**

The entire system ran effectively enough to keep the WPI team competitive with the other US teams. Out of the eight teams that registered for the SPL US Open competition, two teams dropped out to continue developing their code for next year's competition. Of the remaining six teams, WPI placed in fourth.

Improvements to each individual module worked well in conjunction with the other modules. The distance improvements to the vision module and the linear corrections to the odometry data allowed the localization module to determine a more accurate position. The improved localization module, with the addition of goalie detection, allowed the behavior module to make more informed decisions. These localization-based decisions allowed the robot to improve the overall soccer strategies used in a game situation, significantly improving the team's performance.

## 5 Conclusion and Recommendations

This project successfully met almost all of its initial goals. The vision system was significantly improved, providing more accurate range and heading data to the goal posts, and eliminating a large number of false positives. This made the information gathered in the vision module significantly more useful to the localization module.

The localization system was able to determine the robot's position based on sighted goal posts. The particle filter was not optimized enough to be practically used, however it was still successful in determining the robot's position when tested. Its speed and efficiency could be improved by finding ways to increase the number of particles which can be tracked by the filter, and optimizing the filter further for a low memory and processor speed environment. Additional improvements to the localization system as a whole could include the use of field lines for localization, as well as implementing sanity checks by using the relative position of the ball from the goalie compared to the perceived ball position of the player running the algorithm.

Behaviors were improved from the previous year's competition code. The robot could more effectively use localization information in deciding what actions to take, such as which direction would be faster to turn, and when the robot should clear the ball in a general forward direction rather than aim directly at the goal. Role switching with a support role was not fully tested, and future work in role switching is recommended, as this is often the difference between the best teams and the middle-of-the-pack teams.

The motion module was more or less untouched for this project, aside from implementing a linear correction for the robot's odometry data. The code base could be significantly improved by developing a better humanoid walk engine, as well as a library of kicks for different situations. This is a huge endeavor, however, and was outside of the scope of this project.

Despite plans at the beginning of the year to develop a replacement for rUNSWift's visualization tool OffNao, the web visualization tool cannot replace OffNao. The visualization tool was a step in the right direction in terms of creating a new tool that will eventually act as cross-platform tool for developing and testing the robots. Future work on the visualization tool would include allowing users to calibrate the robots directly from the web. Additionally, more work could be done to allow better gathering and logging of data from the robot. Particularly, it would be useful to provide some control to the user via the interface for moving the robot's head during calibration.

Overall, the project was successful. With the current state of the code, the robots could effectively play a game of soccer. The WPI team came in fourth place out of the eight teams initially registered for the RoboCup US Open competition. With a bit more work, the WPI Warrior's standing among the US Standard Platform League teams could certainly improve.

## References

- Aldebaran Robotics. (2012). *Hardware platform - corporate - aldebaran robotics | key features*. 2012, from <http://www.aldebaran-robotics.com/en/Discover-NAO/Key-Features/hardware-platform.html>
- Barrett, S., Genter, K., Hausknecht, M., Hester, T., Khandelwal, P., Lee, J., et al. (2010). *Austin villa 2010 standard platform team report* No. 1). Austin, Texas.
- Brindza, J., Cai, L., Thomas, A., Boczar, R., Caliskan, A., Lee, A., et al. (2010). *UPennalizers RoboCup standard platform league team report 2010* No. 1). Philadelphia, Pennsylvania: University of Pennsylvania.
- Czarnetzki, S., Kerner, S., Urbann, O., Hofmann, M., Stumm, S., & Shwarz, I. (2010). *Nao devils dortmund team report 2010* No. 1). Dortmund: Technische Universitat Dortmund.
- Freeston, L. (2002). *Applications of the Kalman filter algorithm to robot localisation and world modeling*. University of Newcastle, NSW, Australia: Retrieved from <http://www8.cs.umu.se/research/ifer/dl/LOCALIZATION-NAVIGATION/Applications%20of%20the%20Kalman%20Filter%20slgorithm%20to%20robot%20localization%20and.pdf>
- Ivanjko, E., Kitanov, A., & Petrovic, I. (2010). Model based Kalman filter mobile robot self-localization. *InTech*, , 59-90. Retrieved from [http://www.intechopen.com/source/pdfs/10566/InTech-Model\\_based\\_Kalman\\_filter\\_mobile\\_robot\\_self\\_localization.pdf](http://www.intechopen.com/source/pdfs/10566/InTech-Model_based_Kalman_filter_mobile_robot_self_localization.pdf)
- Leonard, J. J., & Durrant-Whyte, H. F. (1991). Mobile robot localization by tracking geometric beacons. *Robotics and Automation, IEEE Transactions on*, 7(3), 376-382. Retrieved from [http://ieeexplore.ieee.org/xpls/abs\\_all.jsp?arnumber=88147](http://ieeexplore.ieee.org/xpls/abs_all.jsp?arnumber=88147)
- Martinez-Gomez, J., Jimenez-Picazo, A., & Garcia-Varea, I. (2009). *A particle-filter-based self-localization method using invariant features as visual information*. Spain: University of Castilla-La Mancha. Retrieved from A particle-filter-based self-localization method using invariant features as visual information
- Negenborn, R. (2003). Robot localization and Kalman filters: On finding your position in a noisy world. (Master of Science, Utrecht University). Retrieved from [http://www.negenborn.net/kal\\_loc/thesis.pdf](http://www.negenborn.net/kal_loc/thesis.pdf)
- Peli, T. (1982). A study of edge detection algorithms. *Computer Graphics and Image Processing*, 20, 1. Retrieved from [http://www.sipl.technion.ac.il/new/Staff/Academic/Malah/Publications/Peli\\_Edge\\_Detection\\_1982.pdf](http://www.sipl.technion.ac.il/new/Staff/Academic/Malah/Publications/Peli_Edge_Detection_1982.pdf)
- Ratter, A., Hengst, B., Hall, B., White, B., Vance, B., Sammut, C., et al. (2010). *rUNSWift team report 2010 robocup standard platform league* No. 1). Sydney, Australia: University of New South Wales.

Rekleitis, I. (2004). *A particle filter tutorial for mobile robot localization* No. TR-CIM-04-02) Centre for Intelligent Machine, McGill University.

RoboCup Technical Committee. (2012). *RoboCup standard platform league (nao) rule draft*. The Robocup Federation.

The Robocup Federation. (2012). *RoboCup. 2012*, from <http://www.robocup.org/>

**Appendix A: RoboCup Standard Platform League Qualification Report**

# **WPI Warriors**

## **Team Description, Standard Platform League 2012**

Irena Cich, Frederik Clinckemaillie, Runzi Gao, David Kent, Benjamin Leone, Miaobo Li, Derek MacNeil-Blackmer, William Mulligan, Ryan O'Meara, Quinten Palmer, Alexander Ryan, and  
Sonia Chernova

Worcester Polytechnic Institute  
100 Institute Rd.  
Worcester, MA 01609 USA

**Abstract.** This paper outlines the organization and architecture of the WPI Warrior's 2012 robotic soccer team developed at Worcester Polytechnic Institute. The team is made up of undergraduates and graduates ranging from freshman level to first year graduates. The team software architecture is based on the rUNSWift 2010 open source code release from the University of New South Wales. This paper reports on the current state of the software development and documents the modifications made to the rUNSWift software architecture.

### **1 Introduction and Statement of Commitment**

The WPI Warriors first competed in the RoboCup Standard Platform League last year. Upon qualification, the team plans to compete in the RoboCup Standard Platform League 2012 competition. The team consists of undergraduate and first-year graduate students, led by Professor Sonia Chernova. This document outlines our current software, as well as our planned research for the upcoming competition.

### **2 Software Architecture Overview**

Our software architecture is based off of the software architecture of the rUNSWift team [2]. We are replacing and modifying modules as we develop. We have developed our own localization and behavior modules. We have modified the vision module and intend to modify the motion engine. We intend to add more to the world model as we add new features, but the main focus of our work this year has been to replace as much of rUNSWift's code with our own code as possible. We have modified rUNSWift's tools for syncing code and are using their OffNao GUI only for calibration, and we have developed our own tools for visualization and compilation. Below is a representation of our software architecture.



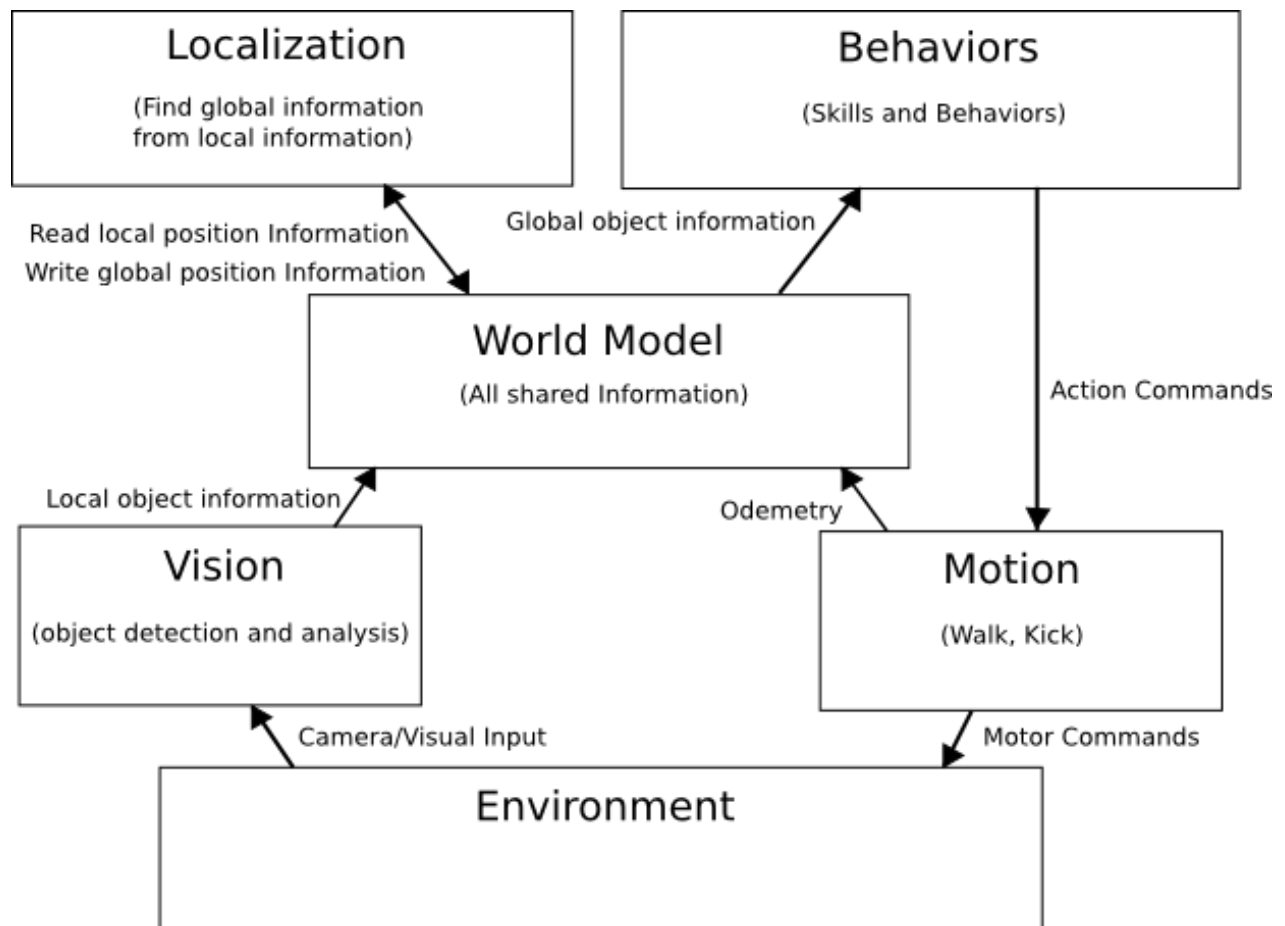


**Figure 44. Software Architecture Overview**

### 3 Vision

The vision module has been modified to increase performance in detecting and analyzing objects. The low level calculations and calibration have remained unmodified, and are based on the rUNSWift architecture [2]. The main priorities in changing the vision module were in the goal detection and analysis. The localization module relies heavily on goal posts, and as such we have worked on optimizing the correct identification of goal posts (i.e. reducing false positives and negatives) and increasing the accuracy of goal post analysis (i.e. correct distance and heading, especially at greater distances).

We plan to add more to the vision module in the future. Our next priority is to implement line detection. This addition would give another input to the localization module. Currently the localization module is heavily reliant on goal post information determined by the vision module, but there are many cases in a game situation where a robot will not see any goal posts. Adding accurate line detection would allow the robot to localize more effectively during these situations.

## 4 Localization

The localization module has been significantly improved upon from the localization module used by the team at the RoboCup 2011 Standard Platform League competition. Previously, the robot performed basic localization based on odometry information and goal post readings. During fall and winter of 2011, the team rewrote the localization module to utilize a particle filter to determine a robot's initial position on the field. Once this initial position is determined, the localization module switches to use Kalman filtering to smooth any positional changes. If the robot loses confidence in its position, the localization module will switch back to the more computationally intensive particle filter to re-establish an initial position for the Kalman filter.

Currently, odometry and goal posts are the only inputs to the localization module. In the coming months, we plan to add rudimentary field line localization to the particle and Kalman filters using the center circle and field line corners.

## 5 Motion

The majority of our motion code utilizes the rUNSWift motion architecture [2]. Our code currently uses a walk generated from rUNSWift's code and a static forward kick that can be mirrored onto either the left or right foot. We plan to improve both the walk engine and our library of kicks before the upcoming competition. Projected improvements to the walk engine include optimizing the motion for use on carpet to prevent overheating of the robot's hip and knee joints, and improving the overall stability of the robot. The team is also developing static sideways and backwards kicks, as well as short-range kicks with low execution times. Goalie blocking motions are also under development.

Another improvement we plan to make for the motion module deals with the current odometry code. The current software uses the same odometry calculation for each robot, despite the fact that all four of our robots have slight differences in their physical motion. To counteract this problem, we plan to implement an odometry configuration file that will correct odometry readings. This would allow each robot to have individual odometry calibration before each game.

## 6 Behavior

The behavior module is the highest-level module in our software architecture. To allow for quick editing, we implement behaviors in Python (rather than the C++ used for all of the lower-level modules). Behaviors are broken down into individual skills, such as scanning with the head, tracking a ball, or aligning on a goal, and behaviors, which implement one or more skills to accomplish a task, such as walking to the ball.

The module uses a finite state machine to determine which behaviors to use in what order. Depending on certain conditions, when a behavior is determined to be finished, it will push itself onto a stack and activate the next appropriate behavior. Each robot role (e.g. striker, goalie, supporter, defender) is defined by a different branching behavior stack. An example stack for a Striker is shown below, where a down arrow represents pushing the current state onto the stack and activating the state below it, and an up arrow represents popping the above state off of the stack.

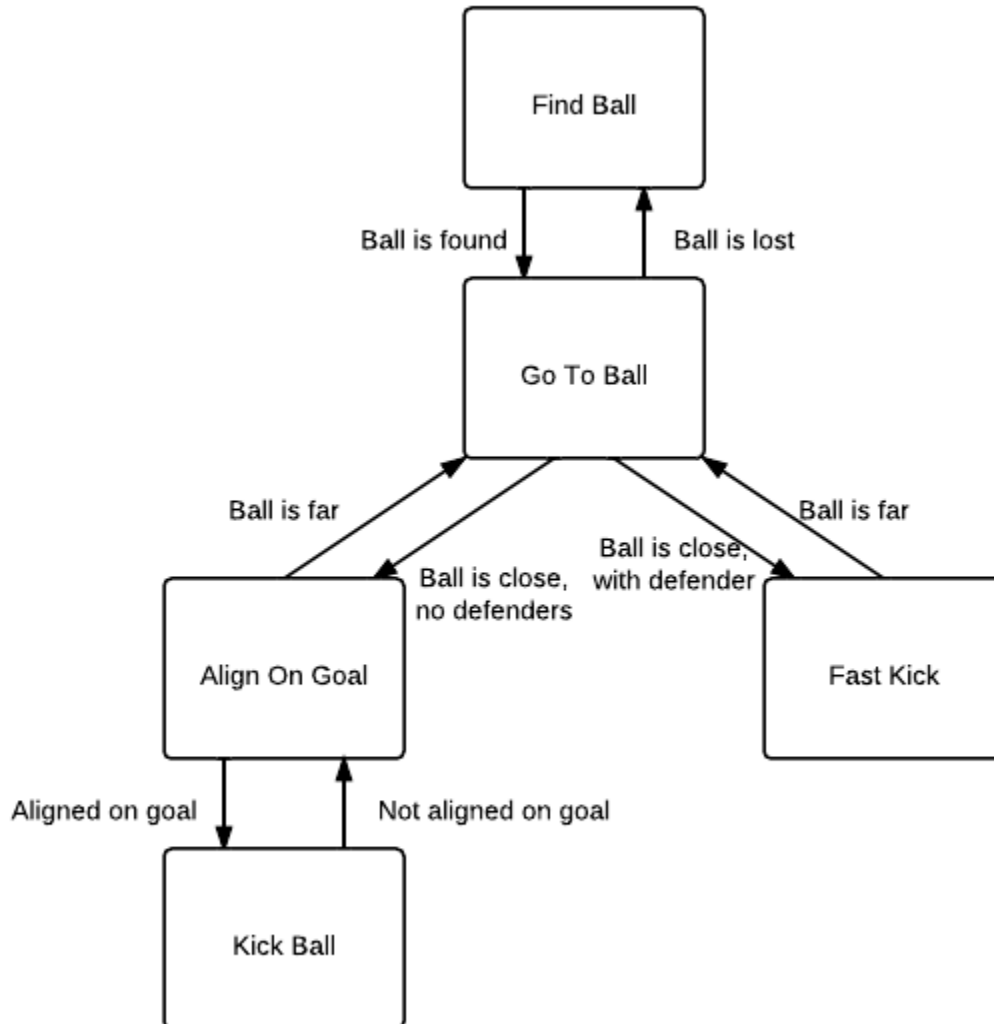


**Figure 45. Striker Behavior Stack Example**

Based on certain conditions, the currently used behavior stack can be switched to the stack of another robot role. For example, if two strikers detect the ball at the same time, the striker that is farther from the ball will switch to the supporter role, leaving the closer striker to get to the ball.

## **7 World Model**

The World Model is where all of the shared information is stored. Vision, Localization, Motion, Behaviors, Game Controller, Receiver, and Trasmitter are the main modules that write to and read from the world model. This module is used to allow each of the modules to communicate with each other, and to maintain an overall representation of the state of the game.

## **8 Acknowledgements**

Special thanks to the University of New South Wales rUNSWift team for making their code available to the research community. We also thank Worcester Polytechnic Institute for financial support for this project.

## **References**

1. Sonia Chernova, Frederik Clinckemaillie, Christopher Conley, Runzi Gao, David Kent, Benjamin Leone, William Mulligan, Khan-Nhan Nguyen, Quinten Palmer. WPI Warriors: Team Description, Standard Platform League 2011.
2. Adrian Ratter, Bernhard Hengst, Brad Hall, Brock White, Benjamin Vance, Claude Sammut, David Claridge, Hung Nguyen, Jayen Ashar, Maurice Pagnucco, Stuart Robinson, Yanjin Zhu. rUNSWift Team Report: Robocup Standard Platform League 2010.